Article:
Luo, G, Ling, N, Xue, C et al. (5 more authors) (2019) Nitrogen-inputs regulate microbial functional and genetic resistance and resilience to drying–rewetting cycles, with implications for crop yields. Plant and Soil, 441 (1-2). pp. 301-315. ISSN 0032-079X

https://doi.org/10.1007/s11104-019-04120-y

Nitrogen-inputs regulate microbial functional and genetic resistance and resilience to drying–rewetting cycles, with implications for crop yields

Gongwen Luo [a], Ning Ling [a], Chao Xue [a], Michaela A. Dippold [b], Les G. Firbank [c], Shiwei Guo [a, *], Yakov Kuzyakov [b,d,e], Qirong Shen [a]

Affiliations:

[a] Jiangsu Provincial Key Lab for Solid Organic Waste Utilization, Jiangsu Collaborative Innovation Center for Solid Organic Waste Resource Utilization, Nanjing Agricultural University, Nanjing 210095, Jiangsu, China

[b] Department of Soil Science of Temperate Ecosystems, Department of Agricultural Soil Science, University of Göttingen, Germany

[c] Faculty of Biological Sciences, University of Leeds, Leeds, UK

[d] Institute of Environmental Sciences, Kazan Federal University, 420049 Kazan, Russia

[e] Agro-Technology Institute, RUDN University, Moscow, Russia

*Corresponding author: Shiwei Guo

Tel.: +86-25-84396393

E-mail: sguo@njau.edu.cn

Abstract

Background and aims The increasing input of anthropogenically-derived nitrogen (N) to ecosystems raises a crucial question: how do N inputs modify the soil microbial stability, and thus affect crop productivity?

Methods Soils from an 8-year rice-wheat rotation experiment with increasing N-input rates were subjected to drying–rewetting (DW) cycles for investigating the resistance and resilience of soil functions, in terms of abundances of genes (potential functions) and activities of enzymes (quantifiable functions), to this stress, and particularly the contribution of resistance and resilience on crop production was evaluated.

Results Although the DW cycles had a stronger effect compared to N fertilization level, the N input was also important in explaining the variation in the resistance and resilience of functional genes and the activities of enzymes involved in C, N and P cycling. Crop yields benefited from both of high resistance and high resilience of soil microbial functions, though the resistance and resilience of soil enzyme activities exhibited a stronger contribution to crop yields compared to the functional genes and the overall contribution strength was conditioned by N input levels.

Conclusions In addition to the well-known direct contribution of N fertilization on crop yields, N input plays an indirect role on crop production via conditioning the resistance and resilience of soil functions in response to repeated DW cycles.

Keywords:

climate change; soil microbial function; resistance and resilience; enzyme patterns; rice-wheat rotation.

Introduction

Soils face various environmental and anthropogenic pressures that alter their functional capacity to fulfil multiple ecosystem services, such as the biogeochemical cycling of elements and supporting crop productivity. To maintain these crucial functions, it is important to understand how soils respond to environmental changes or disturbances (Griffiths and Philippot 2013; Morillas et al. 2015). Current climate trends indicate an increasing number of soil drying-rewetting (DW) cycles resulting from increases in evapotranspiration and soil drought, which have received an increasing attention (Wetherald and Manabe, 2002; Barnard et al. 2013; Székely and Langenheder 2017). Especially in the agricultural soil, the unreasonable management patterns, such as irrigation and crop-rotation can also result in the increase in the numbers of soil DW cycles. The response of soils to such stresses depends on their management and a

combination of both biotic and abiotic soil properties (Griffiths and Philippot 2013; Yuste et al. 2011). Specifically, the functional response of soils is strongly controlled by the intensity and the numbers of DW cycles (Butterly et al. 2009; Meisner et al. 2013), which severely impacts a broad spectrum of microbial processes (Zhao and Running 2010).

Soil moisture is a critical driver of the biogeochemical cycling of carbon (C), nitrogen (N) and phosphorus (P), and influences the transformation of organic matter (Cui et al. 1997; Moyano et al. 2013). These processes are mediated by soil microorganisms through the synthesis and secretion of extracellular enzymes, which have been widely used as sensitive indicators of ecosystem responses to stressors and as a proxy for a potential ecosystem recovery (Daou et al. 2016; Guénon et al. 2013; Hartmann et al. 2015; Loeppmann et al. 2016; Mooshammer et al. 2017; Su et al. 2015). Following a harsh DW cycle, microorganisms must invest energy to regulate osmotic pressure (Landesman and Dighton 2011; Manzoni et al. 2014), and their communities have to reassemble from the dormant or inactive stages, including spores (Székely and Langenheder 2017). The physiological responses of microorganisms and the microbial community re-organisation to soil drying and rewetting cycles require a large investment in resources, which may vary with impact histories and soil properties (Schimel et al. 2007; Székely and Langenheder 2017). Although microbial community composition has been shown to shift in response to DW cycles (Cruz-Martínez et al. 2009; Waldrop and Firestone 2006), many microbial taxonomic groups also exhibit functional redundancy (Kuzyakov et al. 2009). As such, shift in microbial function such as in metabolism or enzyme synthesis may result in overall similar functionality even with an overall different microbial community under altered conditions (Barnard et al. 2013; Morillas et al. 2015; Placella et al. 2012). Microbial functional groups driving organic matter decomposition, N mineralization and nitrification are known to be sensitive to DW cycles (Gao et al. 2016; Guénon et al. 2013; Phillips et al. 2015). However, whether the ability of microbial functions (represented by functional genes and enzymes driving C, N and P cycling) to withstand an external impact (resistance)

and their capacity for recovery to the pre-impact levels (resilience) depends on the management practice and the numbers of the stress event remains uncertain. Additionally, whether functional resistance and resilience may be used as indicators for soil fertility and thus contribute to the crop productivity is not yet clear.

Nitrogen inputs in agroecosystems have increased ten-fold compared to 100 years ago (Canfield et al. 2010). N inputs enhance soil functionality such as biogeochemical cycling and crop production by impacts on microbial activity and nutrient mobilization (Chen et al. 2017; Gallo et al. 2004). N inputs modulate the responses of microbial functions, including functional gene abundances (potential functions) and enzyme activities (quantifiable functions) involved in C, N and P cycling, to the changes in numbers of DW cycles (Francaviglia et al. 2017; Morillas et al. 2015). Therefore, these responses may influence the biological contributions to soil functional resilience and increase the sustainability of farming systems with particular soil types and climatic conditions. We further speculate that agricultural production is not only largely limited by the extent to which agricultural nutrient requirements can be met (Zechmeister-Boltenstern et al. 2011), but also depends on the resistance and resilience of microbial functions to external stresses, including DW cycles, which may also be influenced by long-term N inputs.

The overall objective of this study was, therefore, to characterise the coupled effects between the repeated DW cycles and long-term N inputs on soil microbial functional groups and enzyme activities. We investigated whether the N fertilization modulated the resistance (the ability to withstand the stress) and resilience (the ability to recover from stress) of microbial functions in response to repeated DW cycles, and whether this resistance and resilience further affect soil functions with downstream consequences for crop production. For these purposes, soils from an 8-year rice-wheat rotation experiment with increasing N-input rates (Zhu et al. 2018) was subjected to DW cycles under controlled conditions. Quantitative PCR was employed to quantify the abundance of genes associated with major C, N transformations as well as P mineralization. The details of functional genes are summarized in Table S1.

Additionally, the activities of soil enzymes related to C, N, and P cycling were assessed (see Table S2), and served as functional indicators. We hypothesized that 1) soil function would respond most strongly to the number of DW cycles, however, the level of N fertilization would increase the resistance and resilience of these functions to DW cycling stress; and 2) the N additions' functional buffer to this stress will enhance crop yields.

Materials and Methods

Experimental field site and soil sampling

Field experiments were carried out at the Institute of Agricultural Science Research at Rugao County (32˚44'N, 120˚49'E), Jiangsu Province, China. The fields were used for an annual rotation of winter wheat and summer rice, which is a typical crop production system in areas of Southeast China. The soils of this region are Vertisols developed in fluvial and lacustrine deposits and are also classified as a sandy loam, and the climate displays a high-frequency pattern of DW cycles. The mean annual temperature of this region is approximately 14.7 ℃ with a mean annual precipitation of ~1056 mm. The basic soil physicochemical properties (0-20 cm) at the beginning of the field experiments were : (a) pH, 7.50; (b) total C, 14.5g kg^{-1}; (c) total N, 1.52 g kg^{-1}; (d) available P, 8.40 mg kg^{-1}; and (e) available potassium, 78.4 mg kg^{-1}. The experiment has been in operation since 2010 and includes 5 nitrogen-input levels: 0, 140, 280, 470 and 660 kg N ha^{-1} $year^{-1}$ (termed N0, N140, N280, N470 and N660, respectively) (Table S3). The details for the field treatment design were described previously by Zhu et al. (2018). Crop yields were recorded (Table S4).

On 4 November 2017, soil samples for each N level were collected at a depth of 0-20 cm from all replicate plots. Samples from each plot were composites of 6 randomly located soil cores, which were sieved (<5 mm) to remove visible plant and organic debris. A fraction of each sample was stored at 4 °C for analysing the soil

physiochemical properties and enzyme activities, and another was stored at -20 °C for DNA extraction and other analysis.

Design of DW cycles and soil sampling in the microcosm experiment

Pre-incubation phase

The remaining soils for each N level were subjected to the DW cycles in a microcosm experiment. First, physical, chemical and biological soil characteristics were measured. A pre-incubation period was then used to acclimate the soil microbial communities. The soil from each treatment was wetted to 50% of the water-holding capacity (WHC) (this is equivalent to about 25% soil water content), which is the optimum water content for microbial respiration in soils with similar textures (Setia et al. 2011), and each sample was mixed thoroughly in a plastic bag. This adjustment of soil moisture was relatively small, as the initial water content of the soils was already at or very close to 50% WHC. 50 g soil (dry weight equivalent) was then placed inside each of 20 ventilated canning jars (250 ml) per N treatment, and incubated in the dark at 25 ºC. To avoid soil drying and to allow for gas exchange, the jars were closed using plastic wrap with identical micropores and were weighed daily. Water loss was replaced daily through the addition of the lost mass to ensure that soil moisture remained at 50% WHC. During this pre-incubation, the soil respiration rate stabilised after 14 days (data not shown).

Drying-rewetting phases

At the end of the pre-incubation phase, soils from four randomly selected jars from the 20 from each N treatment were collected and stored at -20 °C for DNA extraction, determination of enzyme activities and other analyses. Soils from another 4 jars were kept at WHC of 50% during the entire course of the experimental period. The remaining soils in the 12 jars were subjected to drying/wetting cycles. The jars were incubated in darkness at 25 °C: the location of the samples within the incubation chamber and the order of samples were randomised. Three DW cycles (with 4 replicates per treatments) were carried out (Fig. 1). Each DW cycle consisted of a 2-week drying phase followed

by a 2-week rewetting phase. We dried soils by removing the plastic wrap and incubating samples at 25 °C under forced air flow (soil moisture content have dropped to <5% WHC). To rewet the soils, we added deionised water using a syringe until the jars attained the weight that corresponded to 50% WHC. During the 2 weeks of the wet stage, soils were maintained at or very close to 50% WHC by weighing. The soils were subjected to different numbers of DW cycles. In the "Constant" treatment (C_0), soils were constantly kept at 50% WHC, while in the "DW1", "DW2" and "DW3" treatments, soils were subjected to one, two, or three DW cycles, respectively. Specifically, DW1 experienced one DW cycle across 4 weeks; DW2 received two DW events across 8 weeks; and DW3 received three DW events throughout the duration of the 12 weeks experiment (experiment timeline is shown in Fig. 1). DW soils were maintained at 50% WHC when not experiencing a DW cycle.

Soils were collected at the end of every DW cycle. One half was immediately stored at -20 °C for subsequent DNA extraction and determination of enzyme activities, and the rest was stored at 4 °C for physicochemical analyses.

Analysis of CO_2 efflux from soil

Total soil CO_2 efflux was determined by the concentration of CO_2 in the headspace of the jars using a gas chromatograph (Agilent 7890A, Agilent Ltd., Shanghai, China). The jar headspace was sampled using a fine needle polypropylene syringe through a rubber septum. We collected 30 ml gas samples from each jar, which were immediately measured. Following each CO_2 sampling, the jars were vented to refresh the headspace and then resealed with plastic wrap until the next gas sampling. We collected samples from the headspace at the start and at the end of the incubation period for each drying and rewetting cycle. Additionally, we considered that consistently rewetting dry soil may produce a large pulse in respiration rates. As such, we also measured the CO_2 concentrations at 1, 2, 3, 5, 8 and 14 days after each rewetting. The initial air CO_2 concentration was used as a blank to subtract from the corresponding CO_2 concentration at the end of the incubation. We calculated fluxes based on the change in CO_2 concentration in the jar, the internal volume of the jar, and the soil dry weight.

Determination of enzyme activities

Soil samples were quickly analysed for enzyme activities (Table S2) by using the MUF-linked model substrates (Deforest 2009; Saiya-Cork et al. 2002) with some modifications. This method, which yields the highly fluorescent cleavage product 4-methylumbelliferyl (MUF) upon hydrolysis, is very sensitive and allows for high-throughput determination of enzyme activities. Briefly, the equivalent of 1.0 g dry mass of fresh soil was added to a 250 ml plastic bottle and homogenised with 100 ml of 50 mM acetate buffer using a polytron homogeniser. Considering that enzyme activity is sensitive to pH, the buffer pH was adjusted to the mean soil pH of the samples within 0.5 units. A magnetic stirrer was used to maintain a uniform suspension. Aliquots (200 µl each) of the soil suspension were placed into 96-well microplates that each contained 50 µl of modified universal buffer at optimal pH levels for the assayed enzyme activities. Subsequently, 50 µl of 200 µM MUF-labelled substrate solutions were added to each well of the microplate. The well contents were mixed by pipetting before the microplates were incubated at 25 °C for 4 h in the dark, following the procedure described by Deforest (2009). The fluorescence intensity was quantified using a microplate fluorometer (Scientific Fluoroskan Ascent FL, Thermo, America) with 365 nm excitation and 450 nm emission filters. Potential enzyme activities were expressed as nanomoles per gram per hour (the detailed calculation procedure is described by Deforest (2009)).

Extraction of soil DNA

Total genomic soil DNA was extracted from 0.25 g of soil per sample (dry weight equivalent) by using a Power Soil® DNA Isolation Kit (Qiagen, Hilden, Germany) according to the manufacturer's protocol. The kit differs from MO BIO's UltraClean® Soil DNA Isolation Kit by including a humic substance/brown colour removal procedure, which effectively removes PCR inhibitors from even the most difficult soil samples. The DNA extracts were purified with a Wizard DNA Clean-Up System (Axygen Bio, USA), as recommended by the manufacturer. DNA quality and quantity were determined spectrophotometrically (NanoDrop 2000, ThermoScientific), and

then replicate extractions were pooled and re-quantified and stored at -20 °C for subsequent analyses.

Quantification of functional gene abundances

Microbial functions were assessed by quantitative PCR of the key genes driving organic matter decomposition, organic P mineralisation and N transformations. Primer sequences for the target genes were adapted for qPCR based on previous studies (Table S1). After running a serial dilution on samples to test for PCR inhibition, the functional gene assay was performed with each sample in triplicate. Standard curves were obtained by using serial dilutions of a known amount of linearized plasmid DNA containing specific gene fragments (Butterly et al. 2016; Luo et al. 2018; Luo et al. 2017). Quantification was performed with an ABI 7500 Cycle Real-time PCR System (Applied Biosystems, Germany) in a 25 µl reaction that included 12.5 µl of SYBR® Premix Ex Taq (2x) (Tli RnaseH Plus), 0.5 µl of ROX Reference Dye II (50x) (TAKARA, BIO, INC, Japan), 0.5 µl of each primer (forward primer and reverse primer), 1 µl of template, and 10 µl ddH_2O to bring the final volume up to 25 µl. The cycling conditions for each gene are listed in Table S1. Our method resulted in slightly different amplification efficiencies for these targeted genes with R^2 values between 0.9916-0.9990 (Table S1). These data were used to correct gene abundance data before statistical analyses.

Calculation of resistance and resilience

The resistance (RS) of each variable was calculated as described by Orwin and Wardle (2004):

$$RS = 1 - \left(\frac{2|D_0|}{C_0 + |D_0|}\right) \quad (1)$$

where D_0 is difference in the value of the response variables between the constant moisture samples (C_0) at the end of each drought period and the treated samples at the end of each drought period (D1, D2 or D3). This RS index increases monotonically with resistance, deals only with absolute differences between controlled and disturbed

soils, and is standardised by the control value to enable valid comparisons between soils. It is bounded by +1 and -1, where an index value of +1 indicates full resistance (i.e., the disturbance did not cause any change in the response variable), an index value of 0 indicates that there was a 100% change in the response variable compared to the control soil, and negative values indicate that there was a change of more than 100% in the response variable compared to the control soil (Orwin and Wardle 2005).

Resilience (RL) was also calculated as described by Orwin and Wardle (2004):

$$RL = \left(\frac{2|D_0|}{|D_x| + |D_0|}\right) - 1 \quad (2)$$

where D_0 is as above and D_X is difference in the values of the response variables between the constant moisture samples (C_0) at the end of each DW cycle and the treated samples (DW1, DW2, DW3) at the end of each DW cycle. This index is standardised by the amount of change initially caused by drought (D_0), as this determines the state from which it has to recover. An index value of 1 indicates that the disturbed soil had completely recovered, and an index value of 0 indicates that either no recovery occurred after the end of the disturbance or that the disturbed soil is now equally different than the control soil but in the opposite direction. A negative value indicates that the disturbed soil is now further away from the control soil than it was initially.

Statistical analyses

Unless otherwise stated, significant differences of the data were determined using ANOVA, and the least significant difference (LSD) test was used to compare the means for each variable ($p < 0.05$). All data were normally distributed based on the skewness and kurtosis coefficients and the visualisation of Q-Q plot tests. The non-metric multidimensional scaling (NMDS) based on Bray-Curtis dissimilarity was performed by using R statistical software to explore differences in microbial functions and enzyme patterns of experimental soils among treatments. We used the following equation to normalise the abundances of C-, N- and P-cycling related genes and the

activities of C-, N- and P-cycling related enzymes belonging to the same functional group (Luo et al. 2018):

$$x' = [\sum_{n=1}^{n}(x_i / \sum_{i=1}^{i} x_i)] / n (i = 1,2,3...; n = 1,2,3...) \quad (3)$$

where x_i is the individual gene abundance or enzyme activity of the sample, i and n indicate the number of samples and genes or enzymes studied, respectively, and x' is the normalised gene abundance or enzyme activity of a certain functional group associated with C, N or P cycles.

Permutational multivariate analysis of variance (PERMANOVA) and two-way ANOVA tests were employed to separate and quantitatively evaluate the effects of N-input levels and the numbers of DW cycles on soil microbial functional capacity (characterized by abundances of functional genes and enzyme activities). Additionally, the similarities (ANOSIM) of potential microbial functions (gene abundances) and enzyme patterns were assessed by using the 'adonis' function in the vegan package of R. A heat-map was generated in R statistical software package to illustrate the independent and interactive effects of N-input levels and DW cycles on the resistance and resilience of individual gene abundances and enzyme activity.

Multiple Regression Analysis was performed in R statistical software to test the individual contribution of resistance and resilience of C-, N- and P-cycling related variables (including functional genes and enzyme activities) on crop yields. Structural equation modeling were constructed to determine whether the N inputs affected the resistance and resilience of soil microbial functions to DW cycles and whether this resistance and resilience further contributed to crop production. The modeling built by coupling factor analysis and path analysis and was run by using AMOS software (IBM SPSS AMOS 20.0.0). The crop yields for the modeling were represented by the annual average yields of wheat and rice in 2017. All of the resistance and resilience of individual genes and individual enzymes were filtered by factor analysis using AMOS software, and then the remaining genes or enzymes (contribution rate >0.50; $p < 0.05$)

were used as the representative parameters describing the total resistance and resilience. The fit of the model was tested by using the maximum likelihood (χ^2) goodness-of-fit test with P-values and the root mean square error of approximation (RMSEA).

Results

CO_2 efflux from soil

The CO_2 production from soils under continuously wet conditions (CW) remained approximately constant across 98 days (Fig. 2). The CO_2 efflux of those with high N input exhibited a high tolerance to drying phases with the recovery of CO_2 efflux occurring more rapidly during rewetting phases. In general, the background CO_2 efflux of soils with high N input show a higher CO_2 efflux than with low N input (Fig. 2).

Functional gene abundances

Quantitative PCR was used to quantify the abundances of genes associated with cellulose degradation (fungcbhIR and GH74), starch degradation (GH31), xylan (or arabinan) degradation (GH51), nitrification (archaeal (amoA-a) and bacterial (amoA-b) ammonia monooxygenase gene), N fixation (nifH), denitrification (narG, nirK, nirS, nosZ and norB), and organic P mineralisation (phoD and BPP). Roughly, the background abundances of functional genes we studied in the N-treated soils were higher than in the N0 soils. The abundances of amoA-a, amoA-b, nirS, narG, nifH, phoD and GH51 genes were the highest in the soil at N660, across the three DW cycles (Fig. S1).

To visualise differences in the patterns of potential microbial functions among the N levels and the DW cycles, multiple gene abundances were employed to compute Bray-Curtis similarity matrices (Fig. 3A). Most of the functional indicators, such as BPP, GH31 and norB genes, contributed strongly to the NMDS ordination of the soils. The NMDS clearly separated the functional gene profiles among the DW cycles along the horizontal axis, and a clear separation of the profiles among the N levels along the

vertical axis ($p < 0.001$; Fig. 3A). The numbers of DW cycles had a greater (76%; $p < 0.001$) impact on the patterns of microbial functional genes than N-input levels (11%; $p < 0.001$), based on PERMANOVA. The interactions between the two factors explained 11% of the total variation (Fig. 3B). Both the DW cycles and N-input levels individually or interactively affected the abundances of individual functional genes (Table S5).

Enzyme activity patterns

In order to visualise the responses of soil functions to the repeated DW cycles, the activities of extracellular enzymes, including α-1,4-glucosidase, β-1,4-glucosidase, β-1,4-xylosidase and β-D-cellobiohydrolase (polysaccharides decomposition), β-1,4-N-acetyl-glucosaminidase and leucine amino peptidase (N assimilation), and phosphatase (organic P mineralization) were assessed. Roughly, the background activities of β-1,4-N-Acetyl-glucosaminidase, phosphatase, α-1,4-Glucosidase, β-1,4-Glucosidase and β-D-Cellobiohydrolase in the N-treated soils were higher than in the N0 soils. The activities of leucine amino peptidase, α-1,4-Glucosidase and β-D-Cellobiohydrolase were the highest in the soils at N470 or N660, across the three DW cycles (Fig. S2).

To visualise differences in the patterns of microbial activity among the N levels and the numbers of DW cycles, multiple enzyme activities were used to compute Bray-Curtis similarity matrices (Fig. 4A). Most of the enzymes contributed strongly to the NMDS ordination of the N fertilization and DW cycles. The NMDS showed a separation of enzyme patterns based on the numbers of DW cycles along the horizontal axis, and based on N levels along the vertical axis (Fig. 4A). Enzyme patterns, from DW1 to DW3, gradually altered from the pre-treatment patterns. Similarly, both DW cycles and N-input levels impacted soil enzymes activities, while DW cycles had a greater (56%, $p < 0.001$) impact than N-input levels (17%, $p < 0.001$). The interactions between these two factors explained 27% of the total variation (PERMANOVA; Fig. 4B). Both the numbers of DW cycles and the N input levels also individually and/or interactively affected the individual enzyme activities (two-way ANOVA; Table S6).

Resistance and resilience of soil functions to DW cycles

Both resistance and resilience exhibited distinct sensitivities between functional genes to the impacts of N-inputs and the DW cycles (Fig. 5). The numbers of DW cycles showed a greater contribution to the variation in resistance and resilience of the amoA-a, nifH, nirS, BPP and norB gene abundances than did N-input levels. The variations in those of the amoA-b, narG, nirK, phoD, fungcbhIR, GH31, GH51 and GH74 gene abundances were mainly attributed to N inputs (Fig. 5).

The numbers of DW cycles showed a greater contribution to the variation in the resistance and resilience of phosphatase, α-1,4-glucosidase, β-1,4-glucosidase, β-1,4-xylosidase and β-D-cellobiohydrolase activities than did the levels of N inputs (Fig. 5). The variations in those of the β-1,4-N-acetyl-glucosaminidase activity were mainly attributed to N inputs (Fig. 5).

Contribution of soil resistance and resilience to crop yields

Multiple regression models were used to predict the impacts of both the resistance and resilience of functional genes and enzymes on crop yields (Fig. 6A; Table S7). The resistance and resilience of soil enzymes to DW cycles had a higher contribution (closer correlation) to crop yields compared with the functional genes. The contribution of N-cycling related enzymes to crop yields was predominantly attributed to resistance (75%, $p < 0.001$), whereas that of C- and P-cycling related enzyme to yields was mainly based on their resilience (71% and 52%, respectively; $p < 0.001$). Structural equation modeling was used to demonstrate the effect pathways of N inputs on crop yields. The modeling (explained over 70% of the total variation in crop yields) predicted the indirect and direct effects of N inputs on crop yields using the influences of the resistance and resilience of soil functional capacity (Fig. 6B). Despite that the contribution of N inputs to crop yield was predominantly due to direct effects, the modeling also showed notable indirect effects via increasing the resistance of functional genes (path coefficient =0.53) and the resilience of enzyme activities (0.64). The indirect effects of N inputs on crop yields were also supported by the resilience of functional genes (-0.72) and the

resistance of enzyme activities (-0.56) (Fig. 6B). These findings suggest that changes in the resistance and resilience of soil enzymes and functional genes were consistent with increases in crop yield along the gradient of increased N input rates (Figs. S3-4).

Discussion

Climate change is predicted to alter precipitation and drought patterns, resulting in more extreme conditions that can impact agricultural productivity in many parts of the world. However, field-based evidence demonstrating the response of soil functions to DW cycles remains very scarce, and, furthermore, is difficult to generalize (Barnard et al. 2013). Here, the results focused on changes in soil functional capacity highlighted the combined effects of long-term N inputs and repeated DW cycles on functional genes (that indicate potential functions) and enzyme activities (that indicate contemporary, quantifiable functions) as well as their resistance and resilience to DW cycles.

Ecological perspective of DW cycles on soil microbial functions

Repeated DW cycles are a principle driver of soil microbial functions involved in C-, N- and P-cycling, including functional gene abundances and enzyme activities (Figs. 3-5). The efficiency of resource use and the physiological strategy of energy allocation by soil microorganisms can control the changes in functional gene abundances and enzyme activities (Guénon et al. 2013; Schimel et al. 2007). Soil resource availability is expected to control the stability of soil microbial functions against DW cycles (Morillas et al. 2015; Schimel et al. 2007). Previously, DW cycles have been shown to induce a large variation in soil nutrient dynamics (Borken and Matzner 2009; Xiang et al. 2008). To investigate the resistance and resilience of soil functions (e.g. nutrient cycles) to DW cycles, it is important to know how soil enzyme activities and functional gene abundances respond to this stress. A soil with high redundancy level of microbial community, that is many species performing a same function, likely act as a buffer against the effect of environmental change on soil functions (Pasari et al. 2013; Strickland et al. 2009). As such, shift in microbial function such as in metabolism or

enzyme synthesis may result in overall similar functionality even with an overall different microbial community under altered conditions (Barnard et al. 2013; Morillas et al. 2015; Placella et al. 2012). These fingdings can explain the results that the resistance and resilience of enzyme activities associated with C and N cycling were more strongly affected by DW cycles than the genes involved in C and N cycling (Fig. 5). Previous studies have indicated that autotrophic nitrification genes (amoA-a and amoA-b) were also abundant in dry soils (Sullivan et al. 2012). The organic matter decomposition genes (such as fungcbhIR) are generally more drought-resilient than corresponding enzymes of organic matter decomposition owing to special microbes with these genes could continue to grow under water stress conditions (Daou et al. 2016; Guenet et al. 2012; Kellner et al. 2007).

Distinct variation between functional gene abundances and enzymes activities in response to the repeated DW cycles (Figs. 3-5, S1-2) indicate that the functional composition of communities (in terms of genes involved in C- N- and P- cycling functions) was highly conserved throughout the disturbation relative to the enzymes activities. Microorganisms can actively synthesize and secrete enzymes to decrease the nutrient limitations by stress (Barnard et al. 2013; Placella et al. 2012). Changes in enzyme activities caused by stress not only strongly depend on the physiology or the function genes of the microbes but also on habitat attributes across DW cycles, e.g. disrupted large macroaggregates (Bünemann et al. 2013). In this study, the resistance and resilience of enzyme activities were strongly affected by an increase in the number of DW cycles (Fig. 5). The resistance of enzyme activities to drought depended on soil nutrient availability and on the direct physical effects of disturbances (Schimel et al. 2007; Morillas et al. 2015; Luo et al. 2017). Inversely, the resilience depends on the survival and proliferation of microbes capable of producing new enzymes (Mooshammer et al. 2017; Waldrop et al. 2000). Hence, the quantifiable functions (in terms of enzymes activities) must have been determined by additional factors that were distinct from the factors shaping the functional structure of communities; that is, soil quantifiable functions and genetic potential function appeared ‘decoupled’ during the

DW cycles.

Nitrogen inputs condition drought-induced change in soil microbial functions

Higher levels of nutrient availability correspond to a greater capacity of the soil to maintain its original biological functions following DW cycles (Morillas et al. 2015). Nitrogen deposition elevated spatial heterogeneity of soil microbial community (Li et al. 2018; Ling et al. 2017). Heterogeneity might enable a population to cope better with an uncertain future (i.e. drought stress), and cells can switch stochastically between the different expression states under this circumstance (Thattai and Van 2004). Stochastic gene expression confers a short-term strategy for survival of individuals that is able to re-populate a community after interferences (Shade et al. 2012), thus it is identified as a key ability for microbial community resistance to pulse stress. Therefore, it is well established that a increase in resistance of microbial functional genes was present in N-amended soils (Figs. 5, S1). Resource allocation processes bring N and P acquisition into stoichiometric balance (Finzi et al. 2011; Ratliff et al. 2015). Soil phosphatase contributes to SOM dephosphorylation and nutrient mineralization (Sinsabaugh 1994; Spohn and Kuzyakov 2013), which supported that phosphatase plays an important role in coupling of C、N and P availability. Thus, the resistance and resilience of soil phosphatase activities and corresponding gene (phoD and BPP) abundances were related to N addition (Figs. 5, S1-2). N addition can aggravate microbial C limitation (Chen et al. 2018), which would be attributed to increased recalcitrant organic matter (alkali insoluble fraction, or humin) through condensation reactions between mineral N and organic matter (Sollins et al. 1996). Such circumstance may increase the relative abundance of microbial species with K-strategy to play a greater contribution on decomposing SOM (Chen et al. 2014). Slow-growing K-strategists tend to be resistant but not resilient to stress (Guénon et al. 2013; Schimel et al. 2007). Thus, these fingdings could explained the negative effect of N inputs on resilience of functional gene abundances (Fig. 6).

High nutrient availability decreases the synthesis of enzymes, a strategy that maintains metabolic balance and energy utilization efficiency of organisms under

repeated DW cycles (Landesman and Dighton 2011; Manzoni et al. 2014). These mechanisms could explain the negative effects of N inputs on the resistance of enzyme activities (Fig. 6). Gene resistance supports the recovering capacity (resilience) of enzyme activities, especially when considering that the increasing extracellular enzymes may be explained by the release of organics into the soil by cell lysis (Daou et al. 2016; Warren and Biochemistry 2016). Thus, N inputs have a positive effect on the resilience of enzyme activities (Fig. 6). Collectively, all these findings suggest that soil functions responded most strongly to the number of DW cycles, however, the level of N input increase the resistance and resilience of these functions to DW cycling stress.

Resistance and resilience of soil functions contribute to crop yields

The contribution of N inputs to crop productivity was found to be primarily caused by direct effects (Fig. 6) (Zechmeister-Boltenstern et al. 2011). Specifically, the model predictions also showed that both of the resistance and resilience of soil microbial functions positively contribute to the increased crop yields (Fig. 6). Short-term bursts in N inputs and microbial mineralisation caused by DW cycles accelerate the cycling of nutrients and energy via affecting soil microbial functions (Fig. 5) (Herrmann et al. 2002; Schimel et al. 1996), and consequently favoring microbial and plant growth (Wang et al. 2010; Wang et al. 2012). This process can remedy the gap of nutrient utilisation and release (Canarini et al. 2015), supporting the long-term stability of crop production. For example, repeated DW cycles of soils often induces not only a substantial pulse in soil respiration but also a leaching of available P (Bünemann et al. 2013). From an ecophysiological perspective, microbes allocate their resource stocks in order to increase the acquisition of nutrient and energy (Bloom et al. 1985). To meet their needs for available P, microorganisms are expected to sacrifice N to get more available P via change at the level of either expression of P-cycling related genes (such as phoD and BPP) or the catalytic efficiency of phosphatases (Allison 2005; Houlton et al. 2008; Luo et al. 2017). Thus, the increase of resistance and resilience of phoD and BPP gene abundances and phosphatase activities to DW cycles could steady P absorption of crops by mediating organic P mineralisation to bioavailable inorganic P

($H_2PO_4^-$ and HPO_4^{2-}).

The potential of soil microbial functions can be equated to the abundance of' functional genes, whereas the implementation of these functions is due to the presence of their catalytic activity (Sinsabaugh et al. 2010). Shift in enzyme synthesis under disturbed conditions can therefore result in overall similar functionality even when the microbial communities are different. The resistance and resilience of soil enzyme activities to DW cycles, therefore, have larger direct effects on crop yields than functional gene abundances (Fig. 6). Indeed, crop yields can benefit from both of high resistance and resilience of soil microbial functions, as showed in the model (Fig. 6). The effects of N inputs on those of microbial functions can be either positive or negative, mainly depending on the changes to enzyme activities (Fig. 6). Both of the resistance and resilience should be maintain at the optimal status in practice for high crop yields, which can be achieved by optimal N inputs. Thus, a balanced nutrient input to agroecosystems is presumably a good recommendation in maintaining soil functionality with consequences for high crop production under altering climatic conditions. Field-based evidence regarding to the optimal N input for targeting high microbial functional stability is needed to further demonstrate and support our predicted results.

Soil biological indicators for soil functional capacity, including functional genes and activities of enzymes associated with C, N and P cycling, were shown to be sensitive to both N-input levels and DW cycles. Although the DW cycles had a stronger effect compared to N fertilization level, the N input was also important in explaining the variation in the resistance and resilience of functional genes and the activities of enzymes involved in C, N and P cycling. Both resistance and resilience of soil functional capacity positively contributed to crop productivity, which can be conditioned by the N input rate. The resistance and resilience of soil enzyme activities exhibited a larger contribution to crop yields compared with the functional gene abundance. In conclusion, N inputs not only meet the nutrient requirements of plant growth directly but also regulate and balance the resistance and resilience of microbial

functions in response to DW cycles, resulting in the regulation of crop production and ecosystem productivity.

Acknowledgements

This work was supported by National Key Research and Development Program of China (2017YFD0200805) and the Special Fund for Agriculture Profession (20150312205).

References

Allison SD (2005) Cheaters, diffusion and nutrients constrain decomposition by microbial enzymes in spatially structured environments. Ecol Lett 8: 626-635.

Barnard RL, Osborne CA, Firestone MK (2013) Responses of soil bacterial and fungal communities to extreme desiccation and rewetting. ISME J 7: 2229-2241.

Bloom AJ, Chapin FS, III, Mooney HA (1985) Resource limitation in plants-an economic analogy. Annu Rev Eco Syst 16: 363-392.

Borken W, Matzner EJ (2009) Reappraisal of drying and wetting effects on C and N mineralization and fluxes in soils. Global Change Biol 15: 808-824.

Bünemann EK, Keller B, Hoop D, Jud K, Boivin P, Plant E (2013) Increased availability of phosphorus after drying and rewetting of a grassland soil: processes and plant use. Plant Soil 370: 511-526.

Butterly CR, Bünemann EK, Mcneill AM, Baldock JA, Marschner PJ (2009) Carbon pulses but not phosphorus pulses are related to decreases in microbial biomass during repeated drying and rewetting of soils. Soil Biol Biochem 41: 1406-1416.

Butterly CR, Phillips LA, Wiltshire JL, Franks AE, Armstrong RD, Chen D, Mele PM, Tang CJ (2016) Long-term effects of elevated CO_2 on carbon and nitrogen functional capacity of microbial communities in three contrasting soils. Soil Biol Biochem 97: 157-167.

Canarini A, Dijkstra FA (2015) Dry-rewetting cycles regulate wheat carbon rhizodeposition, stabilization and nitrogen cycling. Soil Biol Biochem 81: 195-203.

Canfield DE, Glazer AN, Falkowski PG (2010) The evolution and future of earth's nitrogen cycle. Science 330: 192-196.

Chen H, Li D, Zhao J, Zhang W, Xiao K, Wang K (2018) Nitrogen addition aggravates microbial carbon limitation: Evidence from ecoenzymatic stoichiometry. Geoderma 329: 61-64.

Chen J, Chen J, Xiao G, Xiao G, Kuzyakov Y, Kuzyakov Y, Jenerette GD, Jenerette GD, Ma Y, Ma Y (2017) Soil nitrogen transformation responses to seasonal precipitation changes are regulated by changes in functional microbial abundance in a subtropical forest. Biogeosciences 14: 2513-2525.

Chen R, Senbayram M, Blagodatsky S, Myachina O, Dittert K, Lin X, Blagodatskaya E, Kuzyakov YJ (2014) Soil C and N availability determine the priming effect: microbial N mining and stoichiometric decomposition theories. Global Change Biol 20: 2356-2367.

Cruz-Martínez K, Suttle KB, Brodie EL, Power ME, Andersen GL, Banfield JF (2009) Despite strong seasonal responses, soil microbial consortia are more resilient to long-term changes in rainfall than overlying grassland. ISME J 3: 738-744.

Cui M, Caldwell MM (1997) A large ephemeral release of nitrogen upon wetting of dry soil and

corresponding root responses in the field. Plant Soil 191: 291-299.

Daou L, Périssol C, Luglia M, Calvert V, Criquet S (2016) Effects of drying–rewetting or freezing–thawing cycles on enzymatic activities of different Mediterranean soils. Soil Biol Biochem 93: 142-149.

Deforest JL (2009) The influence of time, storage temperature, and substrate age on potential soil enzyme activity in acidic forest soils using mub-linked substrates and l-dopa. Soil Biol Biochem 41: 1180-1186.

Finzi AC, Austin AT, Cleleand EE, Frey SD, Houlton BZ, Walenstein MD (2011) Responses and feedbacks of coupled biogeochemical cycles to climate change: examples from terrestrial ecosystems. Front Ecol Environ 9: 61-67.

Francaviglia R, Renzi G, Ledda L, Benedetti A (2017) Organic carbon pools and soil biological fertility are affected by land use intensity in Mediterranean ecosystems of Sardinia, Italy. Sci Total Environ 599–600: 789-796.

Gallo M, Amonette R, Lauber C, Sinsabaugh RL, Zak DR (2004) Microbial community structure and oxidative enzyme activity in nitrogen-amended north temperate forest soils. Microb Ecol 48: 218-229.

Gao J, Feng J, Zhang X, Yu FH, Xu X, Kuzyakov YJC (2016) Drying-rewetting cycles alter carbon and nitrogen mineralization in litter-amended alpine wetland soil. Catena 145: 285-290.

Griffiths BS, Philippot L (2013) Insights into the resistance and resilience of the soil microbial community. FEMS Microbiol Rev 37: 112-129.

Guenet B, Lenhart K, Leloup J, Giusti-Miller S, Pouteau V, Mora P, Nunan N, Abbadie L (2012) The impact of long-term CO_2 enrichment and moisture levels on soil microbial community structure and enzyme activities. Geoderma 170: 331-336.

Guénon R, Gros R (2013) Frequent-wildfires with shortened time-since-fire affect soil microbial functional stability to drying and rewetting events. Soil Biol Biochem 57: 663-674.

Hartmann M, Frey B, Mayer J, Mäder P, Widmer F (2015) Distinct soil microbial diversity under long-term organic and conventional farming. ISME J 9: 1177.

Herrmann A, Witter E (2002) Sources of C and N contributing to the flush in mineralization upon freeze-thaw cycles in soils. Soil Biol Biochem 34: 1495-1505.

Houlton BZ, Wang YP, Vitousek PM, Field CB (2008) A unifying framework for dinitrogen fixation in the terrestrial biosphere. Nature 454: 327.

Kellner H, Luis P, Buscot F (2007) Diversity of laccase-like multicopper oxidase genes in Morchellaceae: identification of genes potentially involved in extracellular activities related to plant litter decay. FEMS Microbio Ecol 61: 153–163.

Kuzyakov Y, Blagodatskaya E, Blagodatsky S (2009) Comments on the paper by Kemmitt et al. (2008) 'Mineralization of native soil organic matter is not regulated by the size, activity or composition of the soil microbial biomass – A new perspective' [Soil Biology & Biochemistry 40, 61–73]: The biolo. John Wiley & Sons.

Landesman WJ, Dighton J (2011) Shifts in microbial biomass and the bacteria: fungi ratio occur under field conditions within 3 h after rainfall. Microb Ecol 62: 228-236.

Li J, Guo C, Jian S, Deng Q, Yu CL, Dzantor KE, Hui DF (2018) Nitrogen fertilization elevated spatial heterogeneity of soil microbial biomass carbon and nitrogen in Switchgrass and Gamagrass croplands. Sci Rep 8: 1734.

Ling N, Chen D, Guo H, Wei J, Bai Y, Shen Q, Hu SJ (2017) Differential responses of soil bacterial communities to long-term N and P inputs in a semi-arid steppe. Geoderma 292: 25-33.

Loeppmann S, Blagodatskaya E, Pausch J, Kuzyakov Y (2016) Substrate quality affects kinetics and catalytic efficiency of exo-enzymes in rhizosphere and detritusphere. Soil Biol Biochem 92: 111-118.

Luo G, Friman VP, Chen H, Liu M, Wang M, Guo S, Ling N, Shen QR (2018) Long-term fertilization regimes drive the abundance and composition of N-cycling-related prokaryotic groups via soil particle-size differentiation. Soil Biol Biochem 116: 213-223.

Luo G, Ling N, Nannipieri P, Chen H, Raza W, Wang M, Guo S, Shen QR (2017) Long-term fertilisation regimes affect the composition of the alkaline phosphomonoesterase encoding microbial community of a vertisol and its derivative soil fractions. Biol Fert Soils 53: 375-388.

Manzoni S, Schaeffer SM, Katul G, Porporato A, Schimel JP (2014) A theoretical analysis of microbial eco-physiological and diffusion limitations to carbon cycling in drying soils. Soil Biol Biochem 73: 69-83.

Meisner A, Bååth E, Rousk J (2013) Microbial growth responses upon rewetting soil dried for four days or one year. Soil Biol Biochem 66: 188-192.

Mooshammer M, Hofhansl F, Frank AH, Wanek W, Hämmerle I, Leitner S, Schnecker J, Wild B, Watzka M, Keiblinger KM (2017) Decoupling of microbial carbon, nitrogen, and phosphorus cycling in response to extreme temperature events. Sci Adv 3: e1602781.

Morillas L, Roales J, Gallardo A, Lovett GM, Groffman PM (2015) Nitrogen supply modulates the effect of changes in drying-rewetting frequency on soil C and N cycling and greenhouse gas exchange. Global Change Biol 21: 3854-3863.

Moyano FE, Manzoni S, Chenu C (2013) Responses of soil heterotrophic respiration to moisture availability: An exploration of processes and models. Soil Biol Biochem 59: 72-85.

Orwin KH, Wardle DA (2005) Plant species composition effects on belowground properties and the resistance and resilience of the soil microflora to a drying disturbance. Plant Soil 278: 205-221.

Orwin KH, Wardle DA (2004) New indices for quantifying the resistance and resilience of soil biota to exogenous disturbances. Soil Biol Biochem 36: 1907-1912.

Pasari JR, Levi T, Zavaleta ES, Tilman D (2013) Several scales of biodiversity affect ecosystem multifunctionality. P Natl Acad Sci USA 110: 10219-10220.

Phillips LA, Schefe CR, Fridman M, O'Halloran N, Armstrong RD, Mele PM (2015) Organic nitrogen cycling microbial communities are abundant in a dry Australian agricultural soil. Soil Biol Biochem 86: 201-211.

Placella SA, Brodie EL, Firestone MK (2012) Rainfall-induced carbon dioxide pulses result from sequential resuscitation of phylogenetically clustered microbial groups. Proc Natl Acad Sci USA 109: 10931-10936.

Ratliff TJ, Fisk MC (2015) Phosphatase activity is related to N availability but not P availability across hardwood forests in the northeastern united states. Soil Biol Biochem 94: 61-69.

Saiya-Cork, KR, Sinsabaugh RL, Zak DR (2002) The effects of long term nitrogen deposition on extracellular enzyme activity in an acer saccharum, forest soil. Soil Biol Biochem 34: 1309-1315.

Schimel J, Balser TC, Wallenstein M (2007) Microbial stress-response physiology and its implications for ecosystem function. Ecology 88: 1386.

Schimel JP, Clein JS (1996) Microbial response to freeze-thaw cycles in tundra and taiga soils. Soil Biol Biochem 28: 1061-1066.

Setia R, Marschner P, Baldock J, Chittleborough D, Smith P, Smith J (2011) Salinity effects on carbon mineralization in soils of varying texture. Soil Biol Biochem 43: 1908-1916.

Shade A, Peter H, Allison SD, Baho D, Berga M, Buergmann H, Huber DH, Langenheder S, Lennon JT, Martiny JB (2012) Fundamentals of microbial community resistance and resilience. Front Microbiol 3: 417.

Sinsabaugh RL (1994) Enzymic analysis of microbial pattern and process. Biol Fert Soils 17: 69-74.

Sinsabaugh RL, Lauber CL, Weintraub MN, Ahmed B, Allison SD, Crenshaw C, Contosta AR, Cusack D, Frey S, Gallo ME (2010) Stoichiometry of soil enzyme activity at global scale. Ecol Lett 11: 1252-1264.

Sollins P, Homann P, Caldwell BA (1996) Stabilization and destabilization of soil organic matter: mechanisms and controls. Geoderma 74: 65-105.

Spohn M, Kuzyakov Y (2013) Phosphorus mineralization can be driven by microbial need for carbon. Soil Biol Biochem 61: 69-75.

Strickland MS, Osburn E, Lauber C, Fierer N, Bradford MA (2009) Litter quality is in the eye of the beholder: Initial decomposition rates as a function of inoculum characteristics. Funct Ecol 23:

627-636.

Su JQ, Ding LJ, Xue K, Yao HY, Quensen J, Bai SJ, Wei WX, Wu JS, Zhou J, Tiedje JM (2015) Long-term balanced fertilization increases the soil microbial functional diversity in a phosphorus-limited paddy soil. Mol Ecol 24: 136.

Sullivan BW, Selmants PC, Hart SC (2012) New evidence that high potential nitrification rates occur in soils during dry seasons: Are microbial communities metabolically active during dry seasons? Soil Biol Biochem 53: 28-31.

Székely AJ, Langenheder S (2017) Dispersal timing and drought history influence the response of bacterioplankton to drying-rewetting stress. ISME J 11: 1764-1776.

Thattai M, Van OA (2004) Stochastic gene expression in fluctuating environments. Genetics 167: 523.

Waldrop MP, Balser TC, Firestone MK (2000) Linking microbial community composition to function in a tropical soil. Soil Biol Biochem 32: 1837-1846.

Waldrop MP, Firestone MK (2006) Response of microbial community composition and function to soil climate change. Microb Ecol 52: 716-724.

Wang YS, Liu FL, Neergaard AD, Jensen LS, Luxhøi J, Jensen CR (2010) Alternate partial root-zone irrigation induced dry/wet cycles of soils stimulate N mineralization and improve N nutrition in tomatoes. Plant Soil 337: 167-177.

Wang Z, Liu F, Kang S, Jensen CR (2012) Alternate partial root-zone drying irrigation improves nitrogen nutrition in maize (Zea mays L.) leaves. Environ Exp Bot 75: 36-40.

Warren CR (2016) Do microbial osmolytes or extracellular depolymerisation products accumulate as soil dries? Soil Biol Biochem 98: 54-63.

Wetherald RT, Manabe S (2002) Simulation of hydrologic changes associated with global warming. J Geophys Res 107: 1984-2012.

Xiang SR, Allen D, Patriciaa H, Joshuap S (2008) Drying and rewetting effects on C and N mineralization and microbial activity in surface and subsurface California grassland soils. Soil Biol Biochem 40: 2281-2289.

Yuste JC, Peñuelas J, Estiarte M, Garcia-Mas J, Mattana S, Ogaya R, Pujol M, Sardans J (2011) Drought-resistant fungi control soil organic matter decomposition and its response to temperature. Global Change Biol 17: 1475-1486.

Zechmeister-Boltenstern S, Michel K, Pfeffer M (2011) Soil microbial community structure in European forests in relation to forest type and atmospheric nitrogen deposition. Plant Soil 343: 37-50.

Zhao M, Running SW (2010) Drought-induced reduction in global terrestrial net primary production from 2000 through 2009. Science 329: 940.

Zhu C, Tian G, Luo G, Kong Y, Guo J, Wang M, Guo S, Ling N, Shen QR (2018) N-fertilizer-driven

association between the arbuscular mycorrhizal fungal community and diazotrophic community impacts wheat yield. Agr Ecosyst Environ 254: 191-201.

Figure legends

Fig. 1. Schema of the experimental design showing the treatments and sampling timelines. Soil moisture dynamics are shown along with a timeline and sampling for each treatment. Each drying-rewetting (DW) cycle includes a drought period (14 days) and rewetting period (14 days). The hollow arrows represent the sampling points.

Fig. 2. The CO_2 efflux from soil depending on N fertilization in each moisture treatment during incubation. The DW0, DW140, DW280, DW470 and DW660 treatments were subjected to drying-rewetting events and had N0, N140, N280, N470 and N660 fertilization levels respectively. The CW0, CW140, CW280, CW470 and CW660 were kept at constant moisture, and were fertilised at N0, N140, N280, N470 and N660 levels respectively. Asterisks indicate significant differences at $p < 0.05$ and $p < 0.01$ probability levels (* and **, respectively; ns, not significant).

Fig. 3. Panel (A): Nonmetric Multidimensional Scaling (NMDS) analysis of soil C-, N- and P-cycling related gene abundances for the Pre (pre-incubation), DW1 (the first drying-rewetting cycle), DW2 (the second drying-rewetting cycle) and DW3 (the third drying-rewetting cycle) treatments for N fertilization levels. The NIL and NDW indicate nitrogen-input levels and the numbers of DW cycles, respectively. The arrows (bottom left) of the NIL and NDW effects represents the direction of the effects of nitrogen-input levels and the numbers of DW cycles, respectively. The fungcbhIR and GH74 are the bio-markers of cellulose degradation; GH31 is the bio-marker of starch degradation; GH51 is the bio-marker of xylan (or arabinan) degradation; amoA-a and amoA-b are the bio-markers of nitrification; nifH is the bio-marker for N-fixation; narG, nirK, nirS, nosZ and norB are the bio-markers of denitrification; phoD and BPP are the bio-markers of organic P mineralisation. The lengths of the arrows indicate the effect intensities of the response parameters. The description of all these genes is presented in **Table S1**. Panel (B), Permutational Multivariate Analysis of Variance (PERMANOVA) comparing the main and interactive effects of nitrogen-input levels and the numbers of DW cycles on functional gene abundances (999 permutations). Asterisks (***) indicate significant differences at $p < 0.001$ probability levels. N0, N140, N280, N470 and N660 stand for the soils acquiring 0, 140, 280, 470 and 660 kg N ha^{-1} $year^{-1}$ respectively.

Fig. 4. Panel (A): Nonmetric Multidimensional Scaling (NMDS) analysis of soil C-, N- and P-acquisition enzyme activities for the Pre (pre-incubation), DW1 (the first drying-rewetting cycles), DW2 (the second drying-rewetting cycles) and DW3 (the third drying-rewetting cycles) treatments for nitrogen (N) fertilization levels. The arrows (upper left) of the NIL and NDW effects represents the direction of the N-input levels and the numbers of DW cycles, respectively. The NIL and NDW indicate N-input levels and the numbers of DW cycles, respectively. The lengths of the arrows

indicate the effect intensities of the response parameters, including leucine amino peptidase (LAP), β-1,4-N-Acetyl-glucosaminidase (NAG), phosphomonoesterase (PPN), α-1,4-Glucosidase (α-G), β-1,4-Glucosidase (β-G), β-1,4-Xylosidase (β-X) and β-D-Cellobiohydrolase (CBH), all of which are presented in **Table S2**. Panel (B), Permutational Multivariate Analysis of Variance (PERMANOVA) comparing the main and interactive effects of N-input levels and the numbers of DW cycles on soil enzyme patterns (999 permutations). Asterisks (***) indicate significant differences at $p < 0.001$ probability levels. N0, N140, N280, N470 and N660 stand for the soils acquiring 0, 140, 280, 470 and 660 kg N ha^{-1} $year^{-1}$, respectively.

Fig. 5. The heat map illustrates the main and interactive effects of nitrogen-input levels (NIL) and the numbers of DW cycles (NDW) on the resistance and resilience of individual soil C-, N- and P-cycling related gene abundances and enzyme activities, and the sensitivities of individual gene abundance and enzyme activity to NIL and DWF. The gradient colors denote the F values, and the bluer the color, the bigger the F value. The fungcbhIR and GH74 are the bio-markers of cellulose degradation; GH31 is the bio-marker of starch degradation; GH51 is the bio-marker of xylan (or arabinan) degradation; amoA-a and amoA-b are the bio-markers of nitrification; nifH is the bio-marker for N-fixation; narG, nirK, nirS, nosZ and norB are the bio-markers of denitrification; phoD and BPP are the bio-markers of organic P mineralisation. LAP, Leucine amino peptidase; NAG, β-1,4-N-Acetyl-glucosaminidase, PPN, phosphomonoesterase, α-G, α-1,4-Glucosidase, β-G, β-1,4 -Glucosidase, β-X, β-1,4-Xylosidase; CBH, β-D-Cellobiohydrolase. Asterisks indicate significant differences at $p < 0.05$, $p < 0.01$ and $p < 0.001$ probability levels (*, ** and ***, respectively; white fields, not significant).

Fig. 6. Panel (A): Multiple Regression Analysis was employed to test the individual contribution of resistance and resilience of C-, N- and P-cycling related variables (including functional genes and enzyme activities) to crop yields; Panel (B): Structural equation modeling showed that the effects of anthropogenic N inputs on the resistance (RS) and resilience (RL) of soil microbial functional capacity (including C-, N- and P-cycling related microbial groups and enzyme activities) to DW cycles, which further contribute to crop yields. Continuous and dashed arrows indicate the positive and negative effects, respectively. Numbers following the included variables show the explained percentage of their variance by their predictors. Numbers on arrows are standardized path coefficients. The models fit the data well. Stars denote for significance at $p < 0.05$, $p < 0.01$ and $p < 0.001$ probability levels (*, ** and ***, respectively).

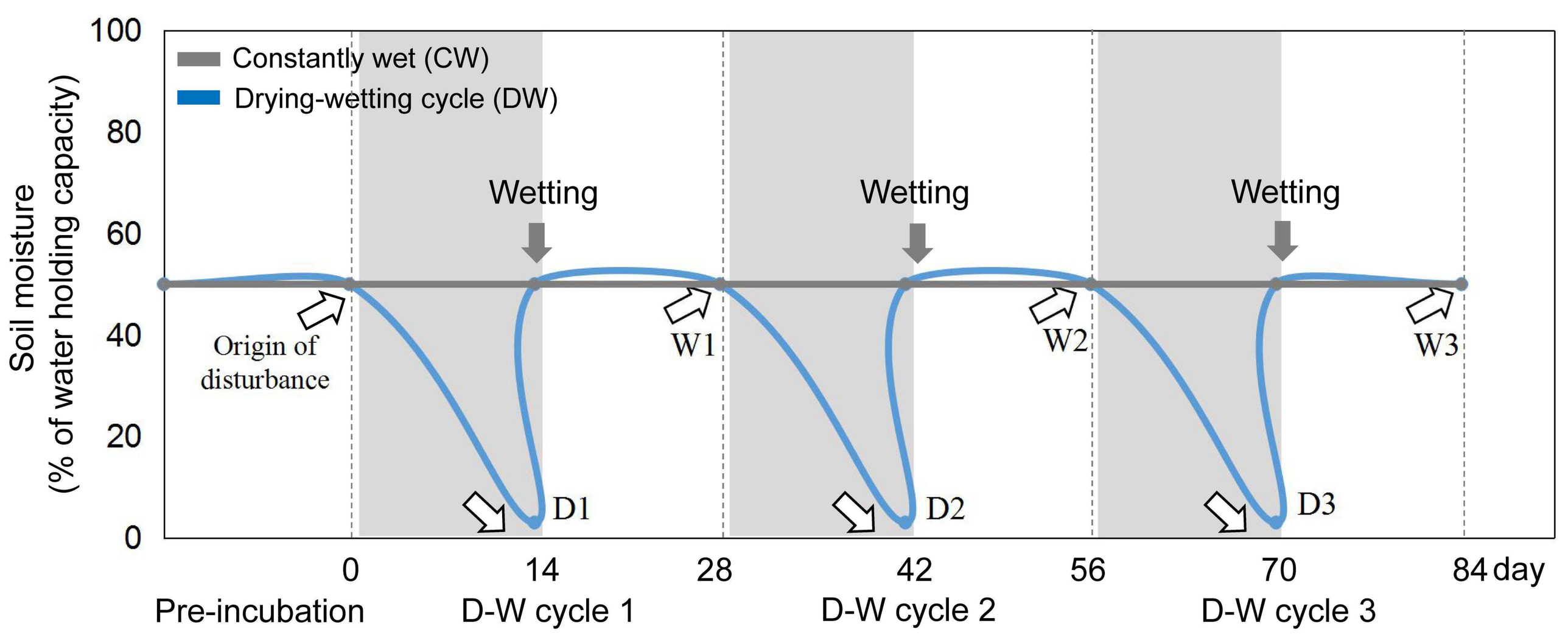
Soil moisture
(% of water holding capacity)
100
80
60
40
20
0
Constantly wet (CW)
Drying-wetting cycle (DW)
Wetting
Wetting
Wetting
Origin of
disturbance
W1
W2
W3
D1
D2
D3
0
14
28
42
56
70
84 day
Pre-incubation
D-W cycle 1
D-W cycle 2
D-W cycle 3

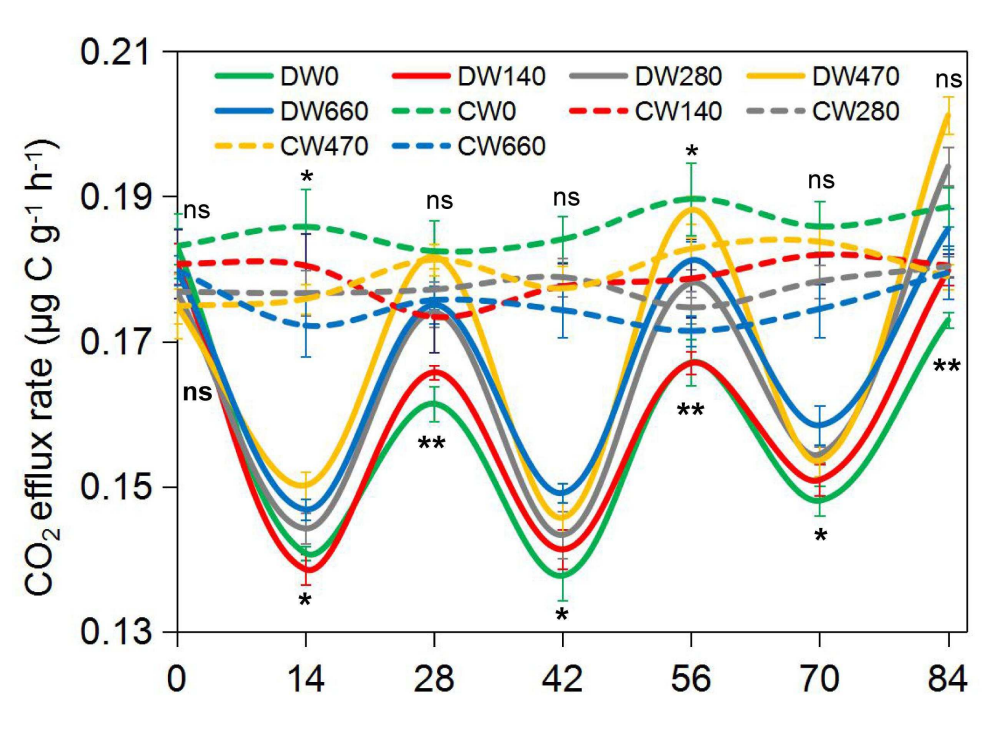
0.21
0.19
0.17
0.15
0.13
CO2 efflux rate (μg C g-1 h-1)
0
14
28
42
56
70
84
DW0
DW140
DW280
DW470
DW660
CW0
CW140
CW280
CW470
CW660
ns
*
**

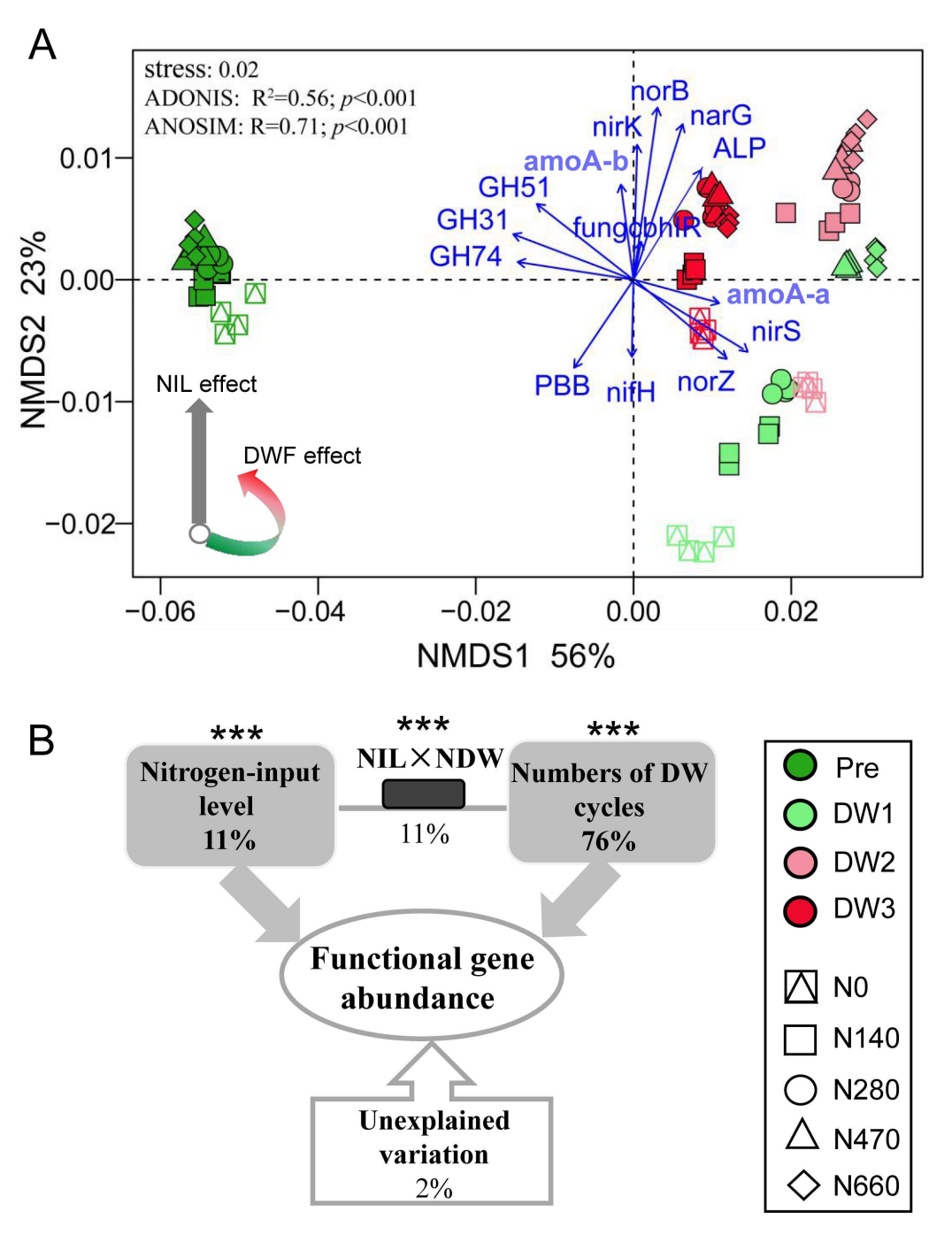
A
stress: 0.02
ADONIS: R²=0.56; p<0.001
ANOSIM: R=0.71; p<0.001
norB
nirK
narG
ALP
amoA-b
GH51
GH31
fungcbhIR
GH74
amoA-a
nirS
PBB
nifH
norZ
NIL effect
DWF effect
NMDS2 23%
NMDS1 56%
0.01
0.00
−0.01
−0.02
−0.06
−0.04
−0.02
0.00
0.02
B
***
Nitrogen-input level 11%
***
NIL×NDW
11%
***
Numbers of DW cycles 76%
Functional gene abundance
Unexplained variation 2%
Pre
DW1
DW2
DW3
N0
N140
N280
N470
N660

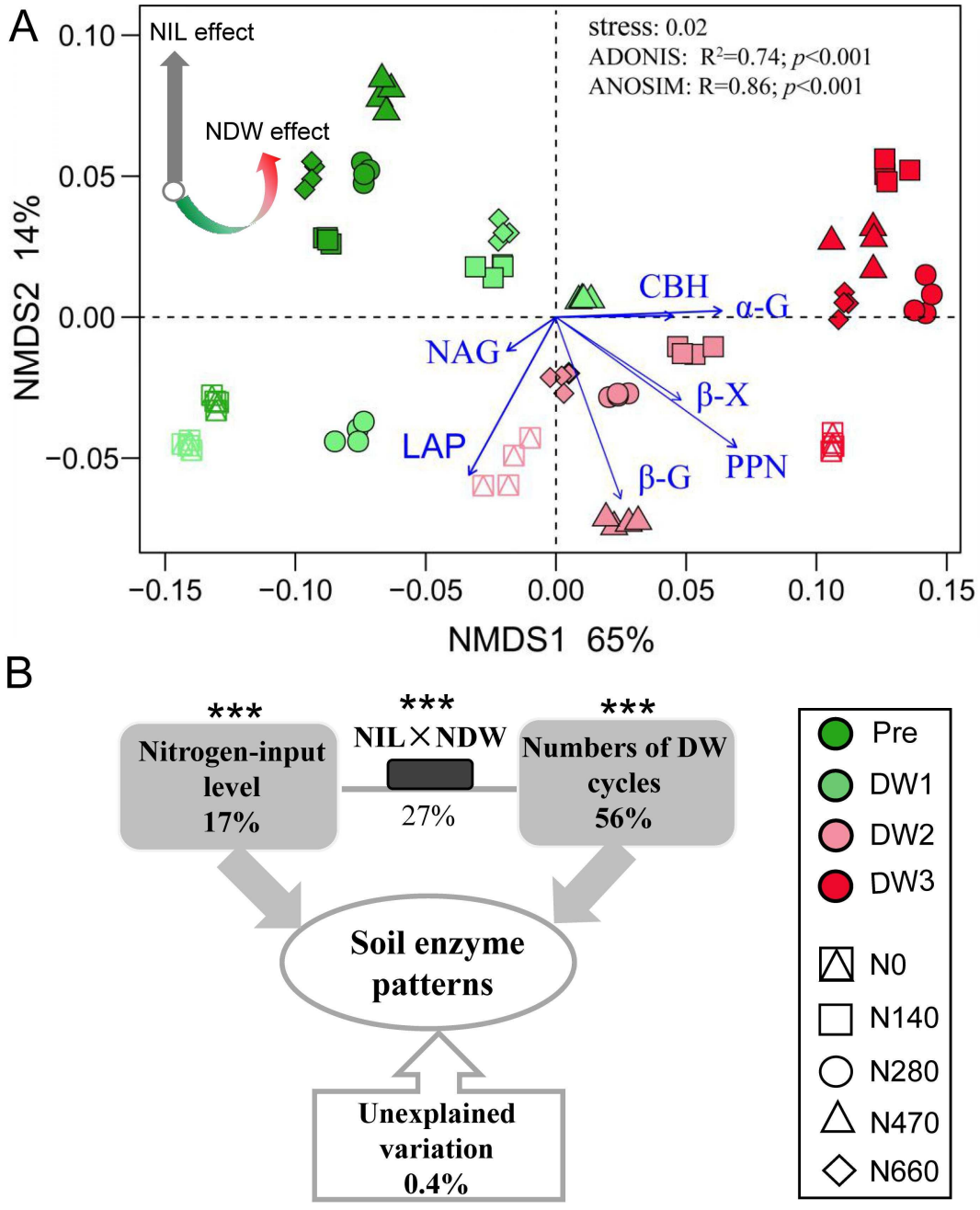
A
NIL effect
NDW effect
stress: 0.02
ADONIS: R²=0.74; p<0.001
ANOSIM: R=0.86; p<0.001
CBH
α-G
NAG
β-X
LAP
PPN
β-G
NMDS2 14%
NMDS1 65%
0.10
0.05
0.00
−0.05
−0.15
−0.10
−0.05
0.00
0.05
0.10
0.15
B
***
Nitrogen-input level 17%
***
NIL×NDW
27%
***
Numbers of DW cycles 56%
Soil enzyme patterns
Unexplained variation 0.4%
Pre
DW1
DW2
DW3
N0
N140
N280
N470
N660

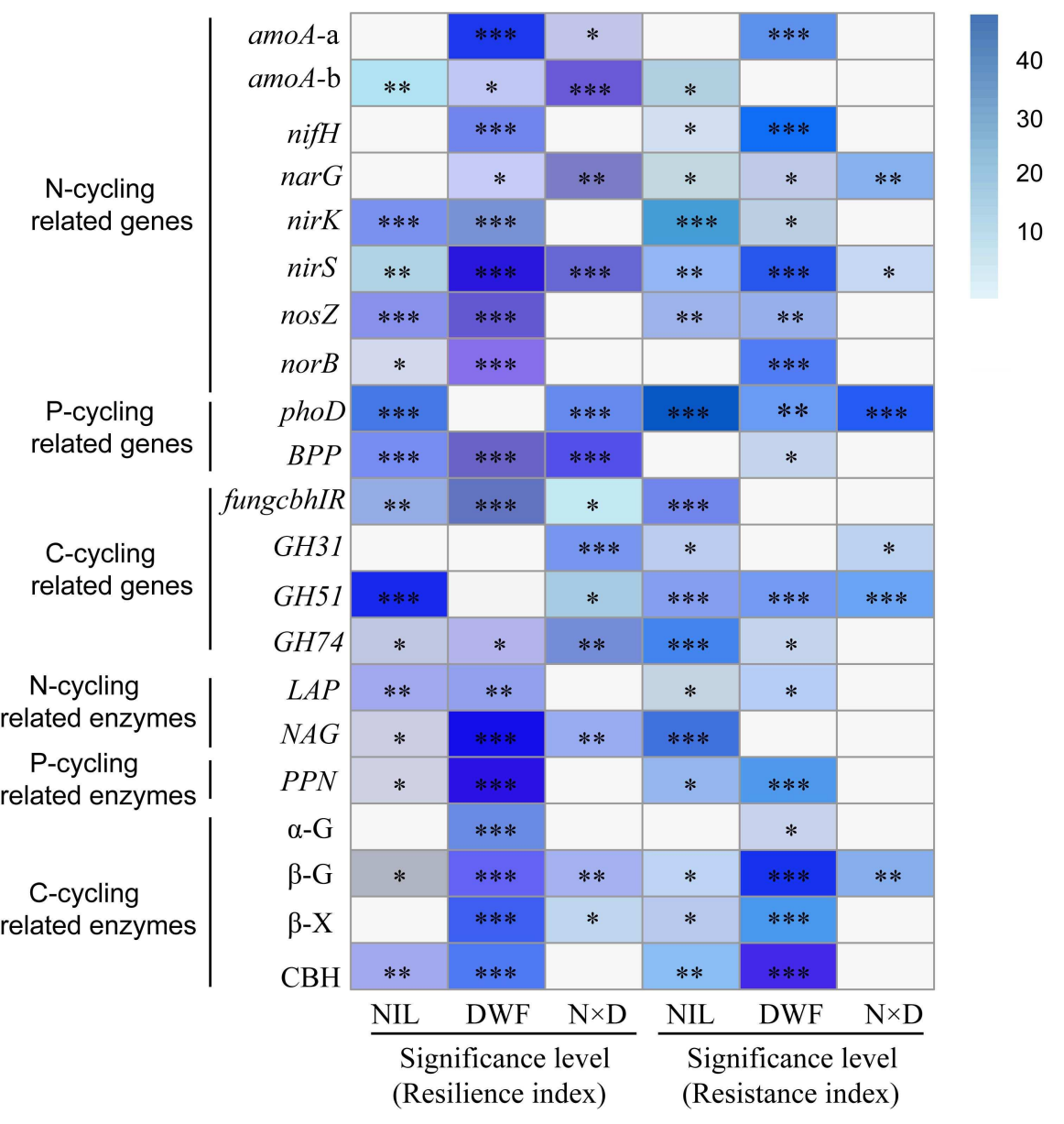
N-cycling related genes
P-cycling related genes
C-cycling related genes
N-cycling related enzymes
P-cycling related enzymes
C-cycling related enzymes
amoA-a
amoA-b
nifH
narG
nirK
nirS
nosZ
norB
phoD
BPP
fungcbhIR
GH31
GH51
GH74
LAP
NAG
PPN
α-G
β-G
β-X
CBH
40
30
20
10
NIL
DWF
N×D
NIL
DWF
N×D
Significance level (Resilience index)
Significance level (Resistance index)

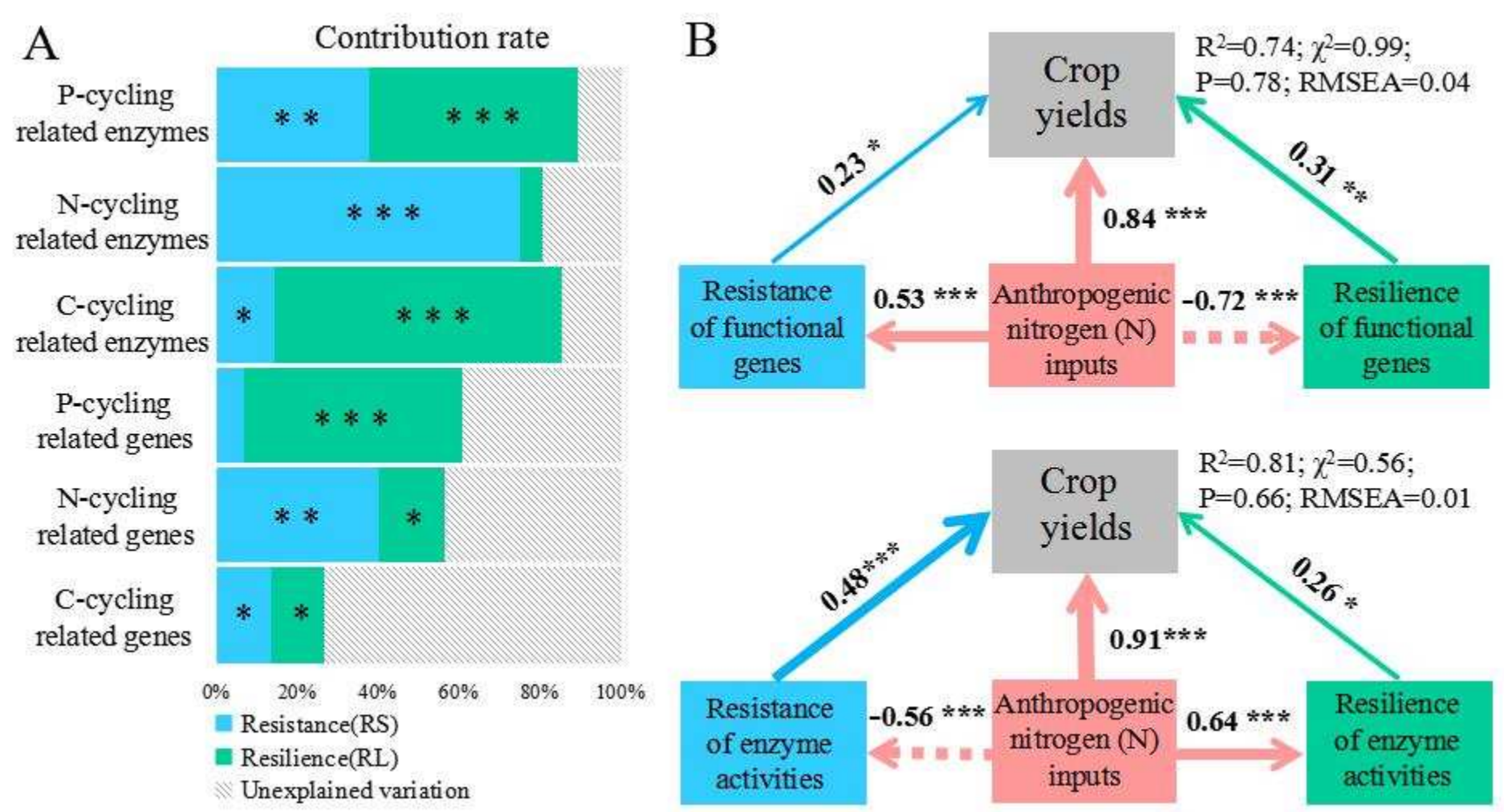
A
Contribution rate
P-cycling related enzymes
N-cycling related enzymes
C-cycling related enzymes
P-cycling related genes
N-cycling related genes
C-cycling related genes
0%
20%
40%
60%
80%
100%
Resistance(RS)
Resilience(RL)
Unexplained variation
B
Crop yields
R²=0.74; χ²=0.99;
P=0.78; RMSEA=0.04
0.23 *
0.84 ***
0.31 **
Resistance of functional genes
0.53 ***
Anthropogenic nitrogen (N) inputs
-0.72 ***
Resilience of functional genes
Crop yields
R²=0.81; χ²=0.56;
P=0.66; RMSEA=0.01
0.48***
0.91***
0.26 *
Resistance of enzyme activities
-0.56 ***
Anthropogenic nitrogen (N) inputs
0.64 ***
Resilience of enzyme activities

Supplementary for:

Nitrogen-inputs regulate microbial functional and genetic resistance and resilience to drying–rewetting cycles, with implications for crop yields

Gongwen Luo [a], Ning Ling [a], Chao Xue [a], Michaela A. Dippold [b], Les G. Firbank [c], Shiwei Guo [a, *], Yakov Kuzyakov [b,d,e], Qirong Shen [a]

Affiliations:

[a] Jiangsu Provincial Key Lab for Solid Organic Waste Utilization, Jiangsu Collaborative Innovation Center for Solid Organic Waste Resource Utilization, Nanjing Agricultural University, Nanjing 210095, Jiangsu, China

[b] Department of Soil Science of Temperate Ecosystems, Department of Agricultural Soil Science, University of Göttingen, Germany

[c] Faculty of Biological Sciences, University of Leeds, Leeds, UK

[d] Institute of Environmental Sciences, Kazan Federal University, 420049 Kazan, Russia

[e] Agro-Technology Institute, RUDN University, Moscow, Russia

*Corresponding author: Shiwei Guo

Tel.: +86-25-84396393

E-mail: sguo@njau.edu.cn

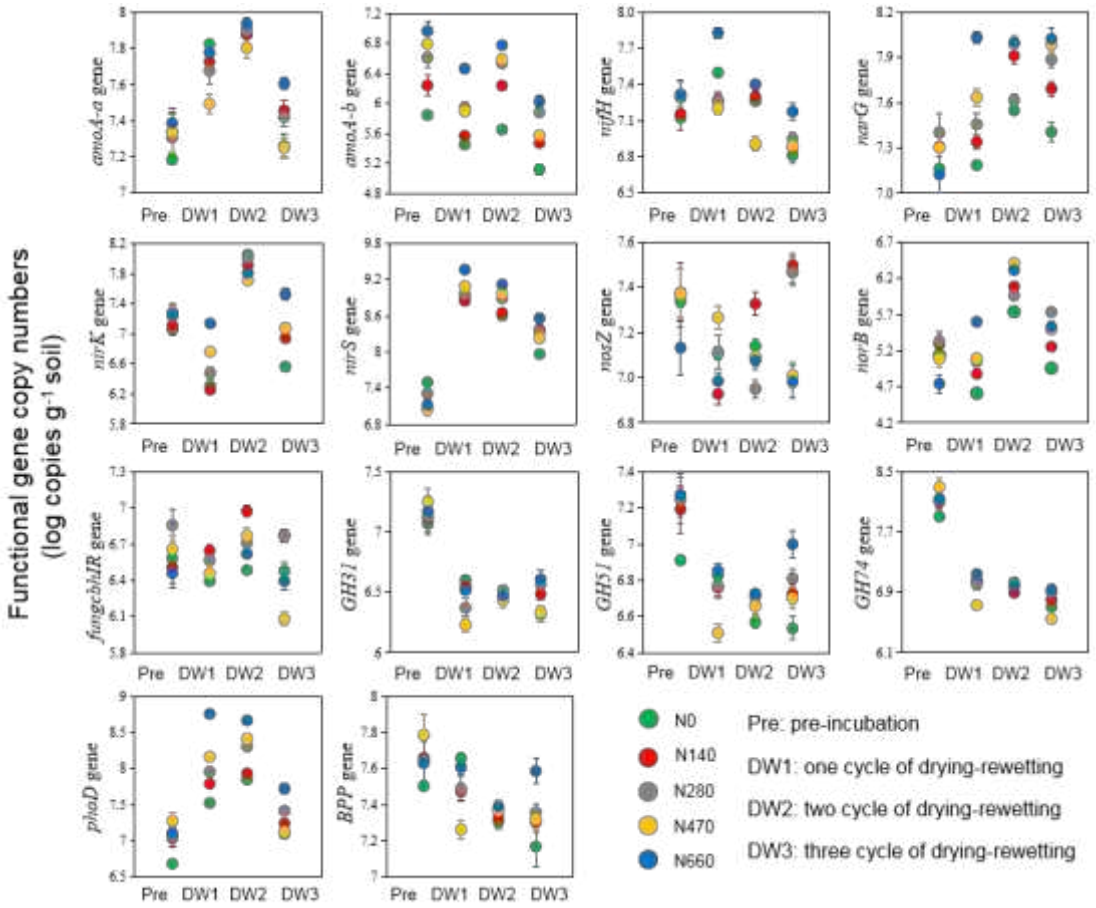

Fig. S1. The abundance of C-, N- and P-cycling genes, including amoA-a (archaeal ammonia monooxygenase gene), amoA-b (bacterial ammonia monooxygenase gene), nirK, nirS, norB, narG, nifH, nosZ, BPP (beta-propeller phytase gene), phoD, fungcbhIR, GH31, GH51 and GH74 (GH: glycoside hydrolase family), based on gene copy numbers that were quantified by quantitative PCR. Bars represent mean ± standard deviation (SD).

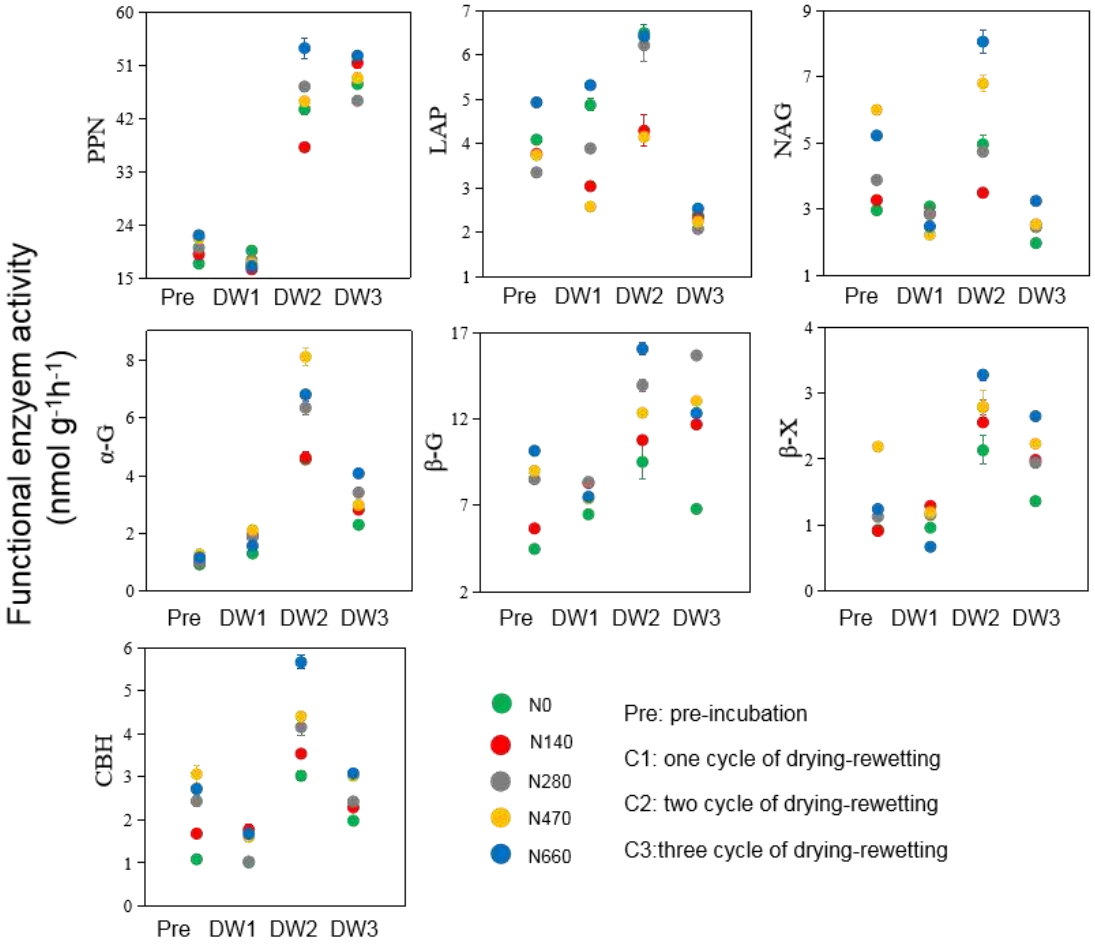

Fig. S2. The activities of the C-, N- and P-acquisition enzymes, including leucine amino peptidase (LAP), β-1,4-N-Acetyl-glucosaminidase (NAG), phosphomonoesterase (PPN), α-1,4-Glucosidase (α-G), β-1,4-Glucosidase (β-G), β-1,4-Xylosidase (β-X) and β-D-Cellobiohydrolase (CBH). Bars represent mean ± standard deviation (SD).

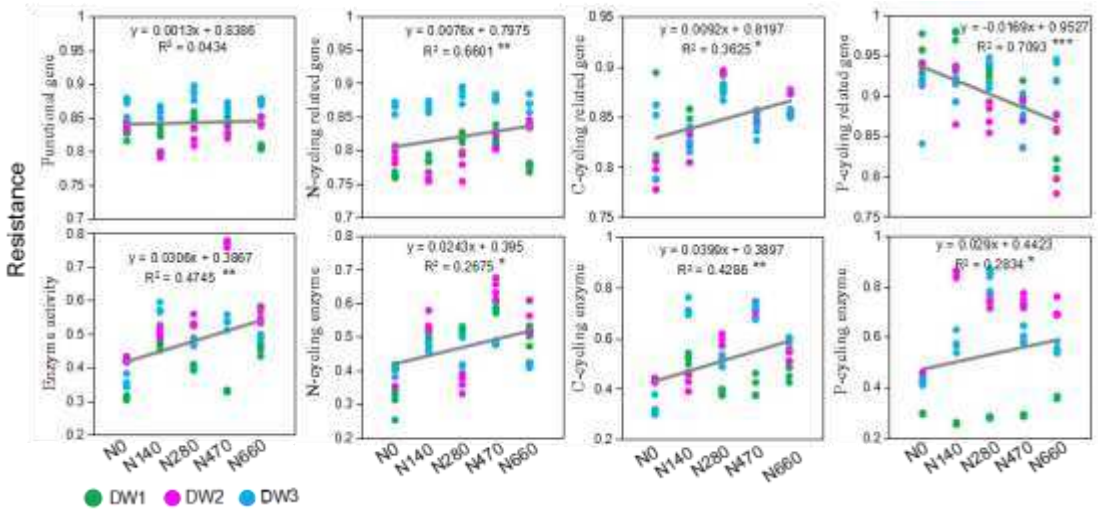

Fig. S3. The models show the overall changes in the resistance of gene abundances and enzyme activities we studied to DW cycles along the gradient of increased rate of N input. DW1, DW2 and DW3 stand for the first, second and third drying-rewetting cycles, respectively.

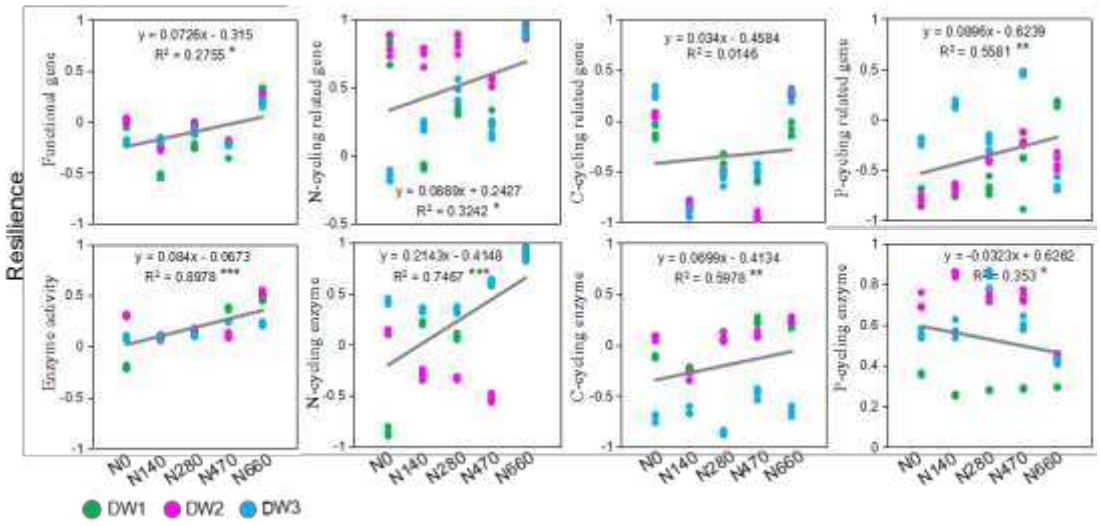

Fig. S4. The models show the overall changes in the resilience of gene abundances and enzyme activities we studied to DW cycles along the gradient of increased rate of N input. DW1, DW2 and DW3 stand for the first, second and third drying-rewetting cycles, respectively.

Table S1. The primers used for quantitative PCR and corresponding amplification cycling conditions.

Primer set	Target gene	Amplicon length (bp)	Amplification efficiencies	Amplification cycling conditions	References
CrenamoA23F (ATGGTCTGGCTWAGACG) CrenamoA616R (GCCATCCATCTGTATGTCCA)	amoA-a	624	98–102%	40 cycle (95 °C 60s, 60°C 5s, 72°C 34s)	Könneke et al. (2005); Long et al. (2012)
Bac-amoA-1F (GGGGTTTCTACTGGTGGT) Bac-amoA-2R (CCCCTCKGSAAAGCCTTCTTC)	amoA-b	491	95–101%	40 cycle (95 °C 60s, 60°C 5s, 72°C 31s)	Rasche et al. (2011); Szukics et al. (2012)
nifHF (AAAGGYGGWATCGGYAARTCCACCAC) nifHRb (TGSGCYTTGTCYTCRCGGATBGGCAT)	nifH	413	90–98%	40 cycle (95 °C 60s, 60°C 5s, 72°C 34s)	Yergeau et al.(2007); Morales et al. (2010)
narG-f (TCGCCSATYCCGGCSATGTC) narG-r (GAGTTGTACCAGTCRGCSGAYTCSG)	narG	110	101–105%	40 cycle (95 °C 60s, 60°C 5s, 72°C 32s)	Kandeler et al. (2009); Bru et al. (2011)
nirK876 (ATYGGCGGVCAYGGCGA) nirK1040 (ATYGGCGGVCAYGGCGA)	nirK	515	95–100%	40 cycle (95 °C 60s, 60°C 5s, 72°C 34s)	Bárta et al. (2010); Bru et al. (2011)
nirSCd3aF (AACGYSAAGGARACSGG) nirSR3cd (GASTTCGGRTGSGTCTTSAYGAA)	nirS	425	99–104%	40 cycle (95 °C 60s, 60°C 5s, 72°C 34s)	Kandeler et al. (2009); Bárta et al. (2010)
nosZ-F (CGCTGTTCITCGACAGYCAG) nosZ-R (ATGTGCAKIGCRTGGCAGAA)	nosZ	380	100–104%	40 cycle (95 °C 60s, 60°C 5s, 72°C 34s)	Rich et al. (2003); Luo et al. (2017a)
cnorB$_B$F (AIGTGGTCGAGAAGTGGCTCTA) cnorB$_B$R (TCTGIACGGTGAAGATCACC)	norB	372	93–97%	40 cycle (95 °C 60s, 60°C 5s, 72°C 34s)	Yu et al. (2014); Luo et al. (2017a)
ALPS-F730 (CAGTGGGACGACCACGAGGT) ALPS-1101 (GAGGCCGATCGGCATGTCG)	phoD	371	93–102%	40 cycle (95 °C 60s, 60°C 5s, 72°C 34s)	Sakurai et al. 2008 Luo et al. (2017b)
BPP-F (GACGCAGCCGA YGAYCCNGCNITNTGG) BPP-R (CAGGSCGCANRTCIACRTTRTT)	BPP	186	94–99%	40 cycle (95 °C 60s, 57°C 30s, 72°C 45s)	Huang et al. (2009); Cotta et al. (2016)
fungcbhIF (ACCAAYTGCTAYACIRGYAA) fungcbhIR(GCYTCCCAIATRTCCATC)	fungcbhIR	100	98–102%	40 cycle (94 °C 30s, 48°C 45s, 72°C 90s)	Edwards et al. (2008); Kellner and Vandenbol (2010)
GH31_350F (CAYCARTGYMGITGGGGNTA) GH31_660R (TTRTCICCNCCCCARTGNCC)	GH31	980	95–100%	40 cycle (95 °C 45s, 50°C 45s, 72°C 100s)	Kellner and Vandenbol (2010)
GH51_280F (AGNTGGCARTGGAAYGCNAC) GH51_350R (ATYTGRTCDATIGCYTGYTG)	GH51	225	96–104%	40 cycle (95 °C 45s, 50°C 45s, 72°C 100s)	Kellner and Vandenbol (2010)
GH74_130F (TTYAARGTIGGIGGNAAYATG) GH74_280R (CCRTCRTAIGGICCNGCNCC)	GH51	460	98–105%	40 cycle (95 °C 45s, 50°C 45s, 72°C 100s)	Kellner and Vandenbol (2010)

GH31, GH51 and GH74 stand for the glycoside hydrolase family 31, glycoside hydrolase family 51 and glycoside hydrolase family 74, respectively. BPP, amoA-a and amoA-b stand for beta-propeller phytase gene, archaeal and bacterial ammonia monooxygenase gene, respectively.

Table S2. Extracellular enzymes with corresponding commission number (EC), corresponding substrate, and the abbreviation used in this study.

Cor. Cycle[1]	Enzyme	Abbreviation	Substrate	EC
C-cycling	α-1,4-Glucosidase	αG	4-MUF[2]-α-D-glucoside	3.2.1.20
	β-1,4-Glucosidase	βG	4-MUF-β-D-glucoside	3.2.1.21
	β-1,4-Xylosidase	βX	4-MUF-β-D-xyloside	3.2.1.37
	β-D-Cellobiohydrolase	CBH	4-MUF-β-D-cellobioside	3.2.1.91
N-cycling	Leucine amino peptidase	LAP	L-Leucine-7-amino-4-methylcoumarin	3.4.11.1
	β-1,4-N-Acetyl-glucosaminidase	NAG	4-MUF-N-acetyl-β-D-glucosaminide	3.2.1.30
P-cycling	Phosphomonoesterase	PPN	4-MUF-phosphate	3.1.3

[1] The enzymes involved in this cycling process

[2] 4-MUF, 4-methylumbelliferyl

Table S3. The fertilization management practices, including application rates and fertilizer types.

Experimental treatments	Amount of nitrogen ($kg \cdot ha^{-1} \cdot y^{-1}$)	Fertilization managements					
		Wheat season			Rice season		
		N ($kg \cdot ha^{-1}$)	P_2O_5 ($kg \cdot ha^{-1}$)	K_2O ($kg \cdot ha^{-1}$)	N ($kg \cdot ha^{-1}$)	P_2O_5 ($kg \cdot ha^{-1}$)	K_2O ($kg \cdot ha^{-1}$)
N0	0	0	75	90	0	90	90
N140	140	50	75	90	90	90	90
N280	280	100	75	90	180	90	90
N470	470	200	75	90	270	90	90
N660	660	300	75	90	360	90	90

N fertilizer: Urea; P fertilizer: Calcium superphosphateand; K fertilizer: Potassium chloride.

Table S4. Soil physical, chemical and biological properties were measured before the start of microcosm experiment, and the crop yields also list in this table.

Nitrogen	pH	EC	NH_4^+-N	NO_3^--N	Alk-N	AP	AK	SOM	Total N	DOC	MBC	MBN	Yield (kg ha^{-1})	
treatments	(H_2O)	(ms cm^{-1})	(mg kg^{-1})	(mg kg^{-1})	(mg kg^{-1})	(mg kg^{-1})	(mg kg^{-1})	(g kg^{-1})	(g kg^{-1})	(mg kg^{-1})	(mg kg^{-1})	(mg kg^{-1})	Rice	Wheat
N0	7.47a	0.23bc	0.86a	13.20c	102.13c	57.14a	90.98a	19.3b	0.84b	66.59c	310.41a	45.60b	5973c	3006c
N140	7.34c	0.22c	0.98a	14.15c	111.23b	45.45b	85.29b	22.26a	1.02a	76.83b	271.78b	56.99a	6611c	3958c
N280	7.40b	0.24b	0.73b	14.71c	112.24b	36.70c	71.35c	22.08a	1.00a	95.71a	187.66d	40.28c	7492b	5758b
N470	7.28d	0.26a	0.63b	17.96b	121.30a	36.15c	64.73c	22.28a	1.01a	87.92a	206.77c	43.88bc	9088a	7948a
N660	7.25e	0.26a	0.71b	25.45a	122.04a	38.33c	64.17c	22.75a	1.03a	91.76a	179.07d	35.72d	8947a	7025ab

[a] Values show replicate plot means and the standard deviation of the mean. Values followed by a different lowercase letter indicate significant differences according to Duncan's LSD test ($p < 0.05$).

Table S5. The main and interactive contributions of nitrogen-input levels (NIL) and numbers of DW cycles (NDW) on the variations of individual functional gene abundance.

Gene	Encoding protein	Functional process	Significance level (Abundance)		
			N-input level	Numbers of DW cycles	NIL×NDW
amoA-a	Ammonia monooxygenase	Nitrification	10.23 **	5.43 *	ns
amoA-b	Ammonia monooxygenase	Nitrification	49.55 ***	45.84 ***	ns
nifH	Nitrogenase Fe protein	Nitrogen fixation	13.43**	28.35 ***	3.65 *
narG	Nitrate reductase alpha	Denitrification	13.72 **	18.77 ***	3.89 *
nirK	Nitrite reductase (Cu)	Denitrification	6.45 *	10.65 **	5.33 *
nirS	Nitrite reductase (cdl)	Denitrification	8.43 **	24.64 ***	ns
nosZ	N_2O reductas	Denitrification	13.43 **	34.45 ***	5.34 *
norB	NO reductase	Denitrification	10.55 **	129.24 ***	ns
phoD	Alkaline phosphomonoesterase	Organic phosphorus mineralization	17.51 ***	8.98 **	ns
BPP	phytase	Organic phosphorus mineralization	10.43 **	88.28 ***	6.00 *
fungcbhIR	cellulolytic enzymes	Cellulose degradation	4.32 *	14.43 **	7.98 **
GH31	α-glucosidases	Starch degradation	ns	106.76 ***	15.32 **
GH51	alpha-L-arabinofuranosidase	Xylan sidechain (arabinan) degradation	10.95 **	58.99 ***	ns
GH74	Endoglucanase or putative xyloglucan-specific endo-b-1,4-glucanase	Cellulose degradation	20.22 **	170.40 ***	4.34 *

GH31, GH51 and GH74 stand for the glycoside hydrolase family 31, glycoside hydrolase family 51 and glycoside hydrolase family 74, respectively. BPP, amoA-a and amoA-b stand for beta-propeller phytase gene, archaeal and bacterial ammonia monooxygenase gene, respectively.

*, ** and *** indicate, $P < 0.05$, $P < 0.01$ and $P < 0.001$, respectively; ns: no significant.

Table S6. The main and interactive contributions of nitrogen-input levels (NIL) and numbers of DW cycles (NDW) on the variations of individual functional gene abundance.

Cor. Cycle	Enzyme	Functional process	Significance level (activity)		
			N-input level	Numbers of DW cycles	NIL×NDW
N-acq.	Leucine amino peptidase	Cleaving of peptide bonds in proteins	13.85 **	4.5 *	ns
	β-1,4-N-Acetyl-glucosaminidase	Hydrolysis of chitooligosaccharides	13.25 ***	5.84 *	ns
P-acq.	Phosphomonoesterase	Cleaving of PO_4^{3-} from P-containing OM	3.85 *	266.68 ***	ns
C-acq.	α-1,4-Glucosidase	Hydrolysis of soluble saccharides	6.26 *	39.35 ***	3.89 *
	β-1,4-Glucosidase	Hydrolysis of cellulose	45.67 ***	79.93 ***	4.33 *
	β-1,4-Xylosidase	Hydrolysis of hemicellulose	12.73 ***	45.29 ***	ns
	β-D-Cellobiohydrolase	Hydrolysis of cellulose	16.92 **	22.90 ***	ns

OM: organic matter; *, ** and *** indicate, $P < 0.05$, $P < 0.01$ and $P < 0.001$, respectively; ns: no significant.

Table S7. The contribution of resistance and resilience of microbial functional groups and enzyme activities to crop yields based on a multiple regression model

Model	p value
Yield = 79555×Resistance-50336×Resilience+154958	$p < 0.001$
Yield = -48346×Resistance-4842×Resilience+33800	$p < 0.001$
Yield = 30378×Resistance-30273×Resilience+2712	$p < 0.001$
Yield = 8790×Resistance-15566×Resilience+10374	$p < 0.001$
Yield = 91396×Resistance-2950×ResilienceL-71765	$p < 0.001$
Yield = -70237×Resistance-6700×Resilience+75645	$p < 0.001$

References

Bárta J, Melichová T, Vaněk D, Picek T, Šantrůčková H (2010) Effect of pH and dissolved organic matter on the abundance of nirK, and nirS, denitrifiers in spruce forest soils. Biogeochemistry 101: 123-132.

Bru D, Ramette R, Saby NPA (2011) Determinants of the distribution of nitrogen-cycling microbial communities at the landscape scale. ISME J 5: 532-542.

Cotta SR, Cavalcante FDA, Seldin L, Andreote FD, Elsas JD (2016) The diversity and abundance of phytase genes (β-propeller phytases) in bacterial communities of the maize rhizosphere. Lett Appl Microbiol 62: 264-268.

Edwards IP, Upchurch RA, Zak DR (2008) Isolation of fungal cellobiohydrolase I genes from sporocarps and forest soils by PCR. Appl Environ Microb 74: 3481-3489.

Huang H, Shi P, Wang Y, et al. (2009) Diversity of beta-propeller phytase genes in the intestinal contents of grass carp provides insight into the release of major phosphorus from phytate in nature. Appl Environ Microb 75: 1508-1516.

Kandeler E, Brune T, Enowashi E, et al. (2009) Response of total and nitrate-dissimilating bacteria to reduced N deposition in a spruce forest soil profile. Fems Microbiol Ecol 67: 444–454.

Kellner H, Vandenbol M (2010) Fungi unearthed: transcripts encoding lignocellulolytic and chitinolytic enzymes in forest soil. PLoS One 5: e10971.

Könneke M, Bernhard AE, Jr DLT, Walker CB, Waterbury JB, Stahl DA (2005) Isolation of an autotrophic ammonia-oxidizing marine archaeon. Nature 437: 543–546.

Long X, Chen C, Xu Z, Oren R, He J (2012) Abundance and community structure of ammonia-oxidizing bacteria and archaea in a temperate forest ecosystem under ten-years elevated CO2. Soil Biol Biochem 46: 163–171.

Luo G, Friman VP, Chen H, et al. (2018) Long-term fertilization regimes drive the abundance and composition of n-cycling-related prokaryotic groups via soil particle-size differentiation. Soil Biol Biochem 116: 213-223.

Luo GW, Ling N, Nannipieri P, Chen H, Raza W, Wang M (2017) Long-term fertilisation regimes affect the composition of the alkaline phosphomonoesterase encoding microbial community of a vertisol and its derivative soil fractions. Biol Fertil Soils 53: 375-388.

Morales SE, Cosart T, Holben WE (2010) Bacterial gene abundances as indicators of greenhouse gas emission in soils. ISME J 4: 799–808.

Rasche F, Knapp D, Kaiser C, et al. (2011) Seasonality and resource availability control bacterial and archaeal communities in soils of a temperate beech forest. ISME J 5: 89–402.

Rich JJ, Heichen RS, Bottomley PJ, Cromack K, Myrold DD (2003) Community composition and functioning of denitrifying bacteria from adjacent meadow and forest soils. Appl Environ Microbiol 69: 5974–5982.

Sakurai M, Wasaki J, Tomizawa Y, Shinano T, Osaki M (2008) Analysis of bacterial communities on alkaline phosphatase genes in soil supplied with organic matter. Soil Sci Plant Nutr 54: 62-71.

Szukics U, Hackl E, Zechmeister-Boltenstern S, Sessitsch A (2012) Rapid and dissimilar response of ammonia oxidizing archaea and bacteria to nitrogen and water amendment in two temperate forest soils. Microbiol Res 167: 103–109.

Yergeau E, Kang S, He Z, Zhou J, Kowalchuk GA (2007) Functional microarray analysis of nitrogen and carbon cycling genes across an antarctic latitudinal transect. ISME J 1: 163–179.

Yu Y, Zhang J, Chen W, Zhong W, Zhu T, Cai Z (2014) Effect of land use on the denitrification, abundance of denitrifiers, and total nitrogen gas production in the subtropical region of china. Biol Fertil Soils 50: 105–113.